

## Carbon quantum dots: recent progresses on synthesis, surface modification and applications

Masoud Farshbaf, Soodabeh Davaran, Fariborz Rahimi, Nasim Annabi, Roya Salehi & Abolfazl Akbarzadeh

To cite this article: Masoud Farshbaf, Soodabeh Davaran, Fariborz Rahimi, Nasim Annabi, Roya Salehi & Abolfazl Akbarzadeh (2018) Carbon quantum dots: recent progresses on synthesis, surface modification and applications, *Artificial Cells, Nanomedicine, and Biotechnology*, 46:7, 1331-1348, DOI: [10.1080/21691401.2017.1377725](https://doi.org/10.1080/21691401.2017.1377725)

To link to this article: <https://doi.org/10.1080/21691401.2017.1377725>



Published online: 21 Sep 2017.



Submit your article to this journal [↗](#)



Article views: 1762



View Crossmark data [↗](#)



Citing articles: 3 View citing articles [↗](#)



## Carbon quantum dots: recent progresses on synthesis, surface modification and applications

Masoud Farshbaf<sup>a</sup>, Soodabeh Davaran<sup>b,c</sup>, Fariborz Rahimi<sup>d</sup>, Nasim Annabi<sup>e,f,g</sup>, Roya Salehi<sup>a,h</sup> and Abolfazl Akbarzadeh<sup>c,i,j</sup>

<sup>a</sup>Department of Medical Nanotechnology, Faculty of Advanced Medical Science, Tabriz University of Medical Science, Tabriz, Iran; <sup>b</sup>Research Center for Pharmaceutical Nanotechnology, Tabriz University of Medical Science, Tabriz, Iran; <sup>c</sup>Joint Ukrainian-Azerbaijan International Research and Education Center of Nanobiotechnology and Functional Nanosystems, Drohobych, Ukraine & Baku, Azerbaijan; <sup>d</sup>Department of Electrical Engineering, University of Bonab, Bonab, Iran; <sup>e</sup>Biomaterials Innovation Research Center, Brigham and Women's Hospital, Harvard Medical School, Cambridge, MA, USA; <sup>f</sup>Harvard-MIT Division of Health Sciences and Technology, Massachusetts Institute of Technology, Cambridge, MA, USA; <sup>g</sup>Department of Chemical Engineering, Northeastern University, Boston, MA, USA; <sup>h</sup>Drug Applied Research Center, Tabriz University of Medical Science, Tabriz, Iran; <sup>i</sup>Stem Cell Research Center, Tabriz University of Medical Sciences, Tabriz, Iran; <sup>j</sup>Universal Scientific Education and Research Network (USERN), Tabriz, Iran

### ABSTRACT

Generally, carbon nanoparticles with a size of 10 nm (or less) are called carbon quantum dots (CQDs, C-dots or CD), which have created huge excitement due to their advantages in chemical inertness, high water solubility, excellent biocompatibility, resistance to photobleaching and various optical superiority. In this article, we describe the recent advancements in the area of CQDs; concentrating on their synthesis techniques, size control, surface modification approaches, optical properties, luminescent mechanism, and their applications in bioimaging, biosensing, drug delivery and catalysis.

### ARTICLE HISTORY

Received 19 July 2017  
Revised 3 September 2017  
Accepted 5 September 2017

### KEYWORDS

Carbon quantum dots; photoluminescent; fluorescent; biomedicine; biosensor; drug delivery

### Introduction

Carbon is generally recognized as a black material and till years ago, it was hard to accept that it could be soluble in water and even exhibit high fluorescence (FL). Nanoscience creates wonderful opportunities for scientific and technological expansions, such as synthesized nanosized carbon structures which possess completely different properties from the macroscopic material [1–5]. Carbon quantum dots (CQDs) are a novel class of carbon nanomaterials with sizes below 10 nm, first found through purification of single-walled carbon nanotubes with preparative electrophoresis in 2004 [6]. CQDs have slowly become a valuable structure in the nano-carbon family, because of being non-toxic, abundant and low-cost nature [7]. The major reason why CQDs have newly attracted huge considerations is due to their strong FL and comparatively better solubility, for which they are referred to as fluorescent carbon [7]. Recently, much development has been accomplished in the preparation, chemical properties and theranostic applications of carbon-based quantum dots [8,9]. CQDs possess superior properties in terms of chemical inertness [9], high solubility [7], easy modification [10] and high resistance to photobleaching [11] compared to traditional semiconductor quantum dots and organic dyes. The premiere biological properties of CQDs, such as

biocompatibility and low toxicity [12], make them proficient for potential applications in biosensing [13], bioimaging [14], photocatalysis [15] and drug delivery [16] (Figure 1). The prominent electronic properties of CQDs as electron givers and acceptors, resulting in electrochemical luminescence (ECL), and chemiluminescence, entrust them with wide potentials in sensors, catalysis and optronics. Apart from their biomedical applications, CQDs are applicable in other industries including solar cells [17] and light-emitting diodes [18]. Furthermore, as anti-fake agents, CQDs were also successfully mixed with commercial inks and reserved their FL in the solid state, features that are promising for solid-state fluorescent sensing, supermarket labelling, object identification, military security and wearable optoelectronics [19]. This article reviews the recent progresses in the area of CQDs, concentrating on their synthesis techniques, size control, modification approaches, optical properties, an overview of luminescent properties, and also highlights their recent applications in bioimaging, biosensing, drug delivery and catalysis subjects.

### Preparation methods

During the last decade, several techniques have been suggested to prepare CQDs, which can be modified through

synthesis or post-treatment. There are some drawbacks facing CQDs preparation, which are required to be noted: (i) agglomeration of CQDs, that could be evaded by applying electrochemical synthesis, and limited solution chemistry techniques, (ii) uniformity and size control, which can be achieved through post-treatment processes such as centrifugation, dialysis and gel electrophoresis and (iii) surface properties which are determinant factors for solubility and specific applications, which can be adjusted through synthesis or post-treatment. In the following sections, we will review the main approaches for CQDs preparation, surface modification and size control of CQDs. A summary of the main advantages and disadvantages of various preparation methods of CQDs is provided in Table 1.

### Electrochemical synthesis

This technique is one of the most prominent top-down methods of producing CQDs using relatively large carbon materials including graphene, graphite, carbon fibre, etc. Advantages of electrochemical method are ease of operation, abundance of raw materials, potential for mass production, low cost and not involving any harsh or toxic chemicals [20,25]. However, tedious purification process of synthesized particles can be considered as a main disadvantage of this method. Electrochemical synthesis of CQDs accomplished when Zhou et al. produced multi-walled carbon nanotubes (MWCNTs) from graphene films by chemical vapour deposition (CVD) [26]. Zhao and Xie reported successful synthesis of CQDs through electrochemical technique in which a graphite column electrode (GE) was electro-oxidized at 3.0 V against a saturated calomel electrode (SCE) with a Pt counter electrode in 0.1 M  $\text{KH}_2\text{PO}_4$  aqueous solution as the supporting electrolyte [27]. Afterwards, the obtained oxidant solution was ultrasonicated, ultra-filtered *via* a 22.0  $\mu\text{m}$  filter membrane and washed with deionized water for three times and dried.

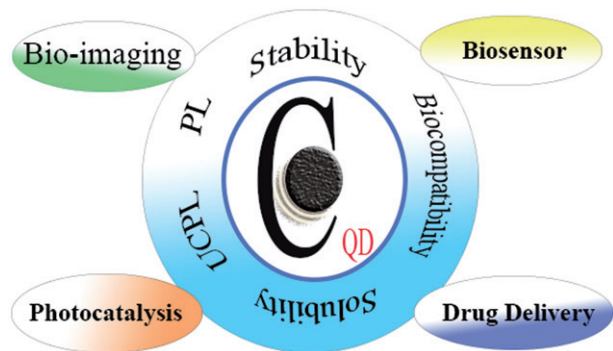


Figure 1. An overview of CQD properties and its applications in biomedicine.

Chi and coworkers produced CQDs *via* electrochemical method using a Pt mesh as counter electrode, an Ag/AgCl as reference electrode and a graphite rod as working electrode assembly plunged in pH 7.0 phosphate buffer solution [28]. Lu et al. obtained a diversity of carbon-based nanoparticles, as well as CQDs from graphite electrode employing ionic liquid-assisted electrochemical exfoliation [29]. Different ratios of water were mixed with 1-methyl-3-butylimidazolium tetrafluoroborate, as the ionic liquid. The graphite rod was located parallel to the Pt wire as counter-electrode in ionic liquid with a separation of 2 cm. The applied potential value was varying from 1.5 to 15 V. Interestingly, the FL of carbon-based nanomaterials including CQDs can be adjusted, ranging from the visible to ultraviolet (UV) region by controlling the water content in the ionic liquid electrolyte [29]. Another electrochemical procedure to produce 1–4 nm CQDs is alkali-assisted electrochemical technique which is reported by Kang and coworkers [30]. It is also possible to produce tiny fragments of graphite by precise cutting of a graphite honeycomb layer into ultra-fine particles, which results in high yield CQDs. This is an easy strategy to produce high-quality CQDs. Applying graphite rods as both anode and cathode and NaOH/EtOH as electrolyte, the same group produced CQDs with a current intensity of 20–190  $\text{mA cm}^{-2}$  (Figure 2). No formation of CQDs was reported in which acids such as  $\text{H}_2\text{SO}_4/\text{EtOH}$  was applied as electrolytes. This indicates that  $\text{OH}^-$  groups are critical and an alkaline environment is the important factor for the producing CQDs by this electrochemical oxidation process.

In another investigation, Canevari et al. reported fabrication of nanocrystalline CQDs based on an electrochemical synthesis method [31]. They applied 1-propanol as carbon source and similar to previous works, they used two Pt electrodes along with an Ag/AgCl electrode as a reference. The reaction was performed in a basic medium by adding of KOH to solution. A constant potential of 6.5 V (100 mA) was applied to the working electrode. The obtained CQDs were collected after 4.5 h and 8.5 h. According to their report, both CQDs produced after 4.5 and 8.5 h showed a similar pattern of spherical geometry with an average diameter of 3 and 4 nm, respectively (Figure 3) [31]. Furthermore, it was revealed that the CQD properties significantly depended on the electrolysis time spent in the process.

Hou et al. also obtained water-soluble functionalized fluorescent CQDs through electrochemical carbonization of sodium citrate and urea [32]. They applied two Pt sheets ( $1.5 \times 2 \text{ cm}^{-2}$ ) as the positive and negative electrodes, with a distance of about 1 cm in a transparent solution containing appropriate proportions of sodium citrate and urea. The procedure was performed at a potential of 5 V (DC) till the

Table 1. The main advantages and disadvantages of various preparation methods of CQDs.

Preparation methods	Advantages	Disadvantages	Ref.
Electrochemical synthesis	Facile, low-cost, without toxic chemicals	Tedious purification process	[20]
Chemical ablation	Tiny particles, accessible precursors	Harsh condition, poor control over size, drastic process	[21]
Supported synthetic technique	Good control over size, uniform and mono-dispersed particles	Time-consuming and multi-step process	[22]
Microwave/ultrasonic synthesis	Facile, low-cost, scalable	Poor control over size	[23]
Laser ablation	Rapid, facile, tunable surface states	Poor control over size, energy consuming, low QY	[24]

transparent solution turned brown (about 1 h). The average size of prepared CQDs was 2.4 nm and possessed good photostability and exhibited a high quantum yield (QY) of 11.9% with a ratio of 1:3 for sodium citrate to urea [32].

### Chemical ablation

This technique applies oxidizing acids to carbonize organic molecules, in which careful control over oxidation can lead to more tiny CQDs [10,21,33,34]. In this method, variety of accessible materials can be applied as precursor. However, the required harsh circumstances and drastic procedures could be disadvantages of this method. Peng and Travas-Sejdic reported a facile aqueous solution based procedure to produce luminescent CQDs using carbohydrates as precursor materials [35]. First, they produced carbonaceous materials *via* dehydrating carbohydrates using concentrated sulphuric acid. Then, the obtained carbonaceous materials were treated with nitric acid and cleaved into tiny CQDs. Finally, as the passivation step, a number of amino-terminated surface

passivation reagents including ethylenediamine, oleylamine, bis(3-aminopropyl) terminated poly(ethylene glycol) (PEG<sub>1500N</sub>) and 4,7,10-trioxa-1,13-tridecanediamine (TTDDA) were investigated. Compared to all passivized CQDs, TTDDA-passivized CQDs showed the highest QY when excited at 360 nm [35]. Surface passivation was the critical step for the photoluminescence (PL) of these CQDs. It was also found that prolonged nitric acid treatment resulted in a blue-shift in the maximum emission wavelength, possibly because of a decrement in the particle size. Nontoxic nature and multicolour emission capabilities of these CQDs make them good candidates in biomedical research. Shen et al. reported synthesis of pH-sensitive photoluminescent CQDs using polyethylenimine (PEI) (25,000 Da), a cationic branched polymer, as both carbon precursor and passivation agent [21]. The CQDs were obtained by refluxing PEI and HNO<sub>3</sub> at 120 °C for 12 h, in which the oxygen-containing carbon core is formed by partial carbonization of PEI with HNO<sub>3</sub>. In the meantime, -COOH groups on the surface of carbon core and the -NH<sub>2</sub> group of PEI caused covalent attachment of PEI to the carbon cores.

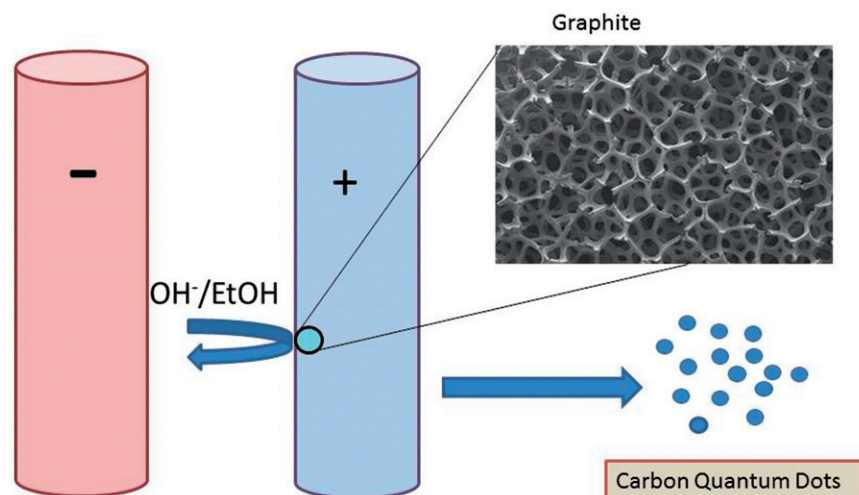


Figure 2. Processing diagram for electrochemical fabrication of CQDs.

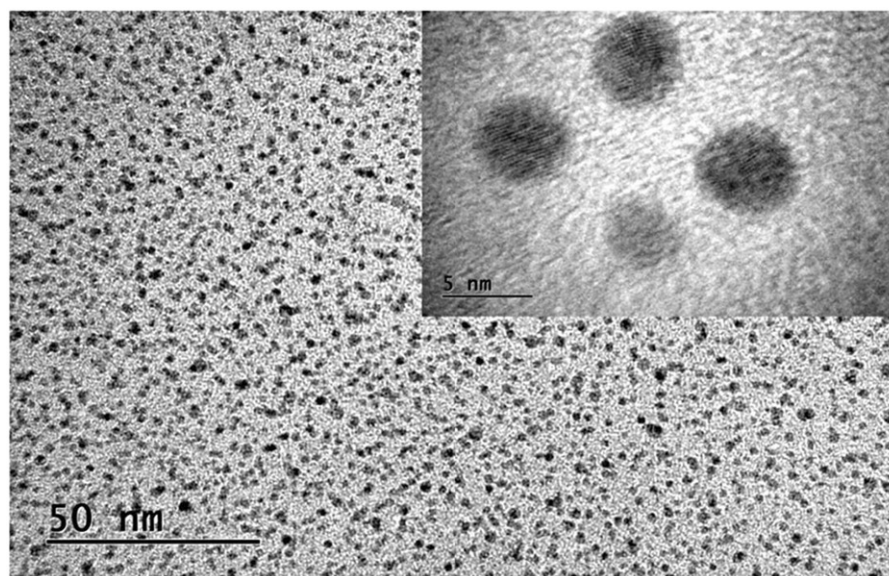
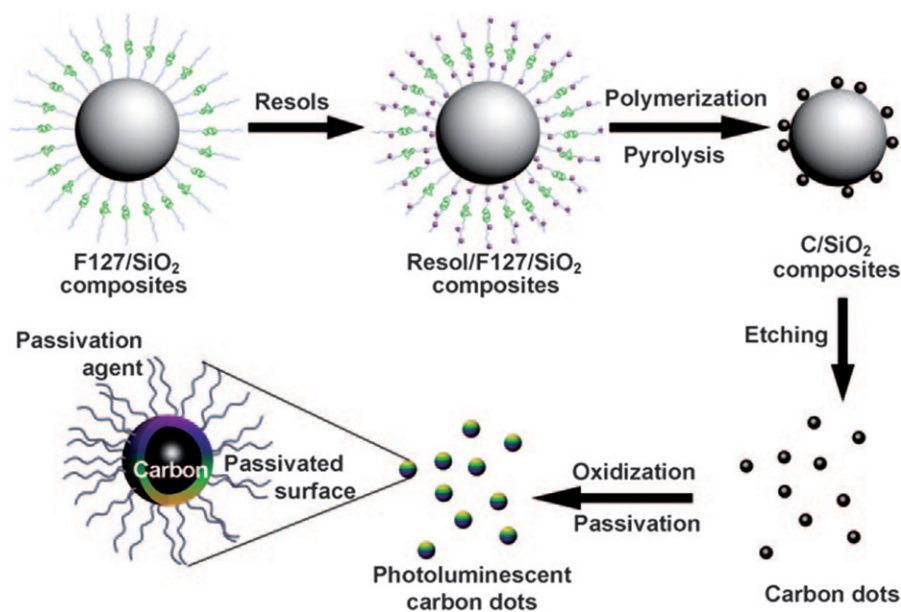


Figure 3. HR-TEM images of CQDs obtained from electrochemical methods. (Reprinted from Ref. [31] Copyright 2016, with permission from Elsevier).



**Figure 4.** Processing diagram for the synthesis of multicolour photoluminescent carbon dots. (Reprinted from Ref. [22] with permission from Copyright 2009 John Wiley and Sons).

It is good to know that the PEI itself is non-emissive as it contains none visible or near-UV chromophores [21]. The PEI-derived CQDs showed reversible pH-sensitive photoluminescent behaviour, in which increasing of pH from 2 to 12, significantly decreased PL.

### Supported synthesis technique

Supported synthetic technique has been commonly used for the preparation of uniform and mono-disperse nanostructures, porous carbon and also CQDs. Liu et al. reported a facile technique to synthesize CQDs (1.5–2.5 nm) by using surfactant (F127)-modified silica spheres (Figure 4) [22]. In the first step, satellite-like polymer/F127/silica composites were produced by an aqueous based technique employing silica colloid spheres functionalized with amphiphilic triblock copolymer F127 (EO<sub>106</sub>PO<sub>70</sub>EO<sub>106</sub>, Mw = 12,600; EO = ethylene oxide, PO = propylene oxide) as carriers and resols (phenol/formaldehyde resins, Mw < 500) as carbon starting material. Thereupon, the nanosized CQDs were obtained by high temperature treatment and removal of silica carriers. Furthermore, acid treatment and simple surface passivation generated water-soluble, multicolour photoluminescent CQDs. Employing surfactant-modified silica nanospheres was the critical step in this method, which prevented the aggregation of the nanosized CQDs through pyrolysis. This method required no elaborate equipment. Therefore, this wet-chemistry-based procedure was suggested to be a flexible economical technique for synthesis of photoluminescent CQDs [22]. In another study, Bourlinos et al. reported synthesis of 4–6 nm CQDs employing thermal oxidation of a properly ion-exchanged Na Y zeolite [36]. This technique led to semi-spherical carbon-based nanoparticles attached onto the external surfaces of the zeolite (CQD-ZEO), maintaining its exchange properties and structural integrity. Therefore, these hybrids incorporate the PL of the supported CQDs with the

unique properties of zeolites. In brief, the synthesis procedure includes ion-exchanging NaY zeolite with 2, 4-diaminophenol dihydrochloride followed by thermal oxidation at 300 °C in air, in which the exchange is performed generally near the external surfaces of the zeolitic crystallites. Therefore, oxidation causes nanoparticles to reside mostly at the external surface of the zeolite matrix. Further, the zeolite matrix can be removed by etching of the obtained (CQD-ZEO) structure with hydrofluoric acid [36]. This method possesses a few advantages: (i) it directly results in oxygen-containing modified CQDs with precisely engineered surface properties and (ii) a better control of shape, size and physical properties is attainable by proper election of the carbon precursor and surface modifier. Zhu and coworkers reported a facile and novel route for synthesis of hydrophilic CQDs employing impregnation technique with mesoporous silica (MS) spheres as nanoreactors and citric acid as the carbon starting material [37]. One of the major advantages of this method was that the obtained CQDs emitted strong blue luminescence and showed excellent upconversion luminescence properties unlike other unpassivized hydrophilic CQDs. Afterwards, the obtained MS spheres (with average particle diameter of 1.3 μm and average pore size of 3.60 nm) were saturated with a mixed solution of complex salts and citric acid. Consequently, nanosized hydrophilic CQDs were obtained by calcination and elimination of MS supports. It is obvious that MS spheres play a critical role as supports, which not only preclude the aggregation of the CQDs, but also restrain the CQDs with narrow size distribution in the pores of MS spheres.

### Microwave/ultrasonic synthesis

This technique has been a very significant procedure in synthetic chemistry and offers different advantages such as being non-toxic, facile, scalable and low-cost. However, poor

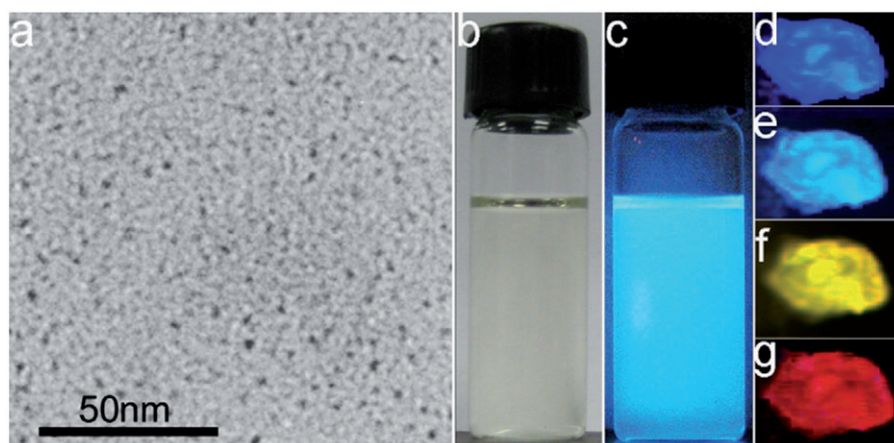


**Figure 5.** (a) TEM image of 5 nm-CQDs obtained from glucose; (b, c) photographs of CQDs dispersals in water with visible light and UV (365 nm, centre) illumination, respectively; (d–g) fluorescent microscope images of CQDs under diverse excitation: d, e, f and g for 360, 390, 470 and 540 nm, respectively. (Reprinted from Ref. [11] Copyright 2011, with permission from Elsevier).

control over size of obtained particles is one of its main disadvantages [23]. Edison et al. developed a rapid and simple microwave technique for preparation of fluorescent nitrogen-doped carbon dots (n-CQDs) using L-ascorbic acid (AA) and  $\beta$ -alanine (BA) as the carbon starting material and the nitrogen dopant, respectively [38]. Briefly, a mixture of AA (3 g) and BA (1 g) was prepared in 30 ml DI water. The obtained mixture was then transferred into a 100 ml Teflon equipped vessel, put in microwave reaction system and heated (900 W) for 1 h at 180 °C. Subsequently, the vessel was cooled down to room temperature and the mixture was ultra-centrifuged with 15,000 rpm for 15 min followed by a cellulose acetate membrane-assisted dialysis process in DI water for 24 h. The obtained n-CQDs showed robust blue FL at 401 nm and the QY of n-CQDs is reported to be about 14% [38]. In another investigation, one-step green microwave-assisted synthesis of wool-derived fluorescent CQDs is reported by Wang et al. [39]. In this work, a solution of tiny pieces of wool (0.3 g) and 40 ml DI water was prepared, then poured into a microwave digestion tank and heated at 200 °C for 60 min by microwave irradiation. This method is not only simple and facile, but also needless to any additives, such as acids, bases or salts for further intricate post-treatment process to purify the CQDs. Yang et al. developed a low-cost and one-step microwave approach for synthesis of water-soluble CQDs with average diameter of 4 nm, in which folate receptor (FR) and folic acid (FA) served as carbon precursors [40]. A proper amount of FA and FR were added to distilled water and heated for 8 min in 500 W microwave oven. The solution colour changed from yellow to brown and finally dark-brown clustered solid, during the process, which indicated the formation of CQDs. The solution was then centrifuged and filtered through a 0.22  $\mu$ m membrane to eliminate agglomerated particles. The prepared particles showed intense PL and possessed high QY of about 25%. Furthermore, FA molecules in the CQDs let them to be taken by FA-receptor-positive cancer cells, which renders them as a new biocompatible probe to distinguish FA-receptor-positive cancer cells from normal cells in biological imaging and cancer diagnosis [40].

Another simple way to prepare CQDs (less than 5 nm) from glucose or active carbon by employing a one-step alkali

or acid assisted ultrasonic treatment technique was explored by Li et al. [11]. In this method, they first prepared 1 mol/l solution of glucose in deionized water and then added HCl (50 ml, 36–38 wt.%) into the solution of glucose. After that, the mixed solution was ultrasonicated for 4 h. Finally, the pure solution of CQDs acquired from glucose/HCl was oven-dried at 80 °C for 6 h. A bright and colourful PL could be emitted from such mono-dispersed water-soluble fluorescent CQDs, which covers the whole visible to (near infrared) N-IR spectral range (Figure 5). In particular, the N-IR emission of CQDs can be attained by N-IR excitation. Additionally, the CQDs possessed great up-conversion fluorescent properties and the results showed that the particle surfaces were rich in hydroxyl groups, that gave them high hydrophilicity [11].

A facile microwave-assisted hydrothermal (MAH) technique was employed to prepare water-miscible crystalline CQDs with an average size of 1.65 nm, in which glucose was applied as carbon precursor [41]. This technique combined both the benefits of hydrothermal and microwave methods and required no surface passivation agents. The only substance was glucose derived from fructose or sucrose. The glucose molecules were pyrolysed and then transformed to CQDs as shown in Figure 6(a). The PL QY of obtained particles were about 5–7% and they showed intense UV emission of 4.1 eV, which is the shortest emission wavelength amongst all the solution-based QDs [41]. In this technique, the microwave heating offers both fast heating and homogeneous process, that results in narrow size distribution of CQDs. The protocol is followed by preparing different glucose concentrations (2.2, 4.4, 6.7, 8.9 and 11.1 wt.%) and heated by a typical microwave oven at various powers (280, 336, 462, 595 and 700 W) for a period of time (1, 3, 5, 7, 9 and 11 min). It turned out that the experimental parameters such as source concentration, heating time and microwave power have a distinct effect on the size of final CQDs.

### Laser ablation

Laser ablation is facile, eco-friendly and effective method which is applied for production of carbon-derived nano-materials including CQDs in which the surface states of

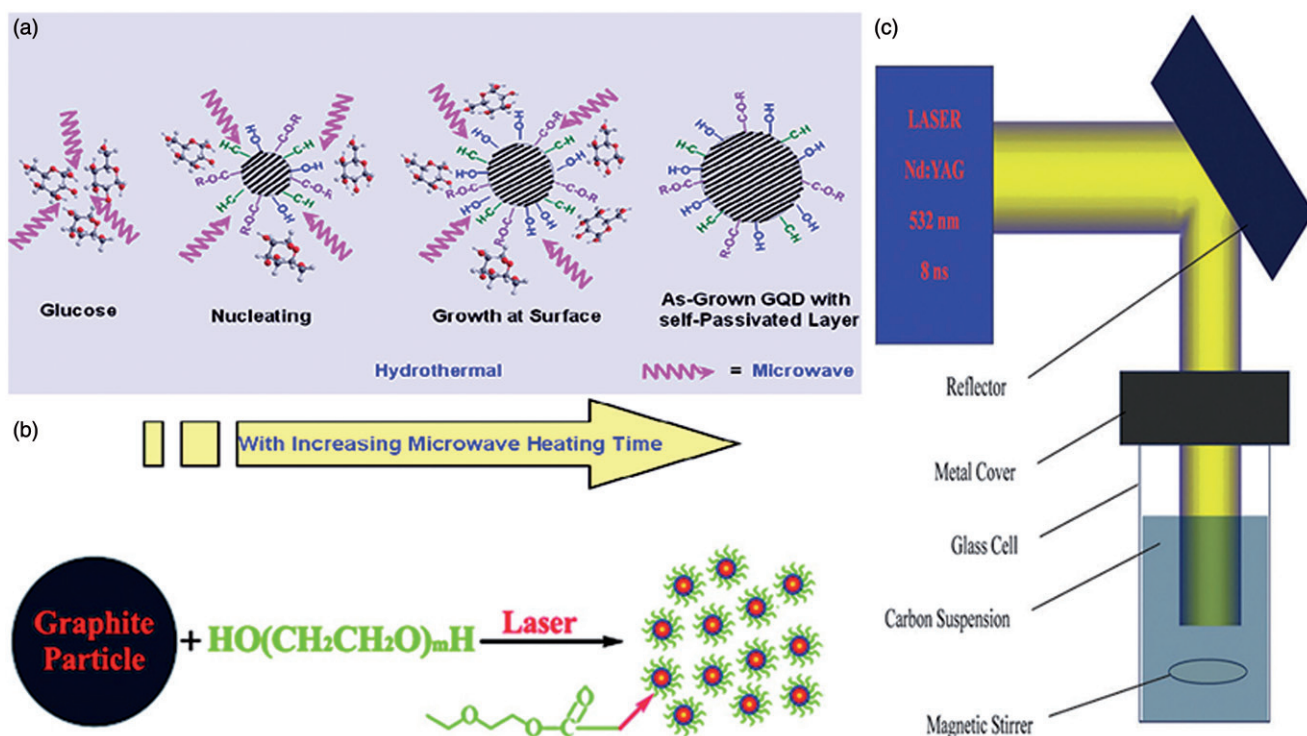


**Figure 6.** (a) Schematic depiction of producing of CQDs by MAH technique. (Reprinted with permission from Ref. [41] Copyright (2012) American Chemical Society); (b) processing diagram of the one-step preparation of luminescent CQDs in PEG200N solvent (Reprinted with permission from The Royal Society of Chemistry); (c) schematic representation of laser ablation experimental setup. (Reprinted from Ref. [45] with permission from The Royal Society of Chemistry).

particles are tunable. Recently, Li and colleagues prepared CQDs by laser ablation of a carbon target in a water vapour company with a carrier gas (argon) at 75 kPa and 900 °C [14,42–46]. CQDs with bright luminescence emission were obtained after refluxing in  $\text{HNO}_3$  for up to 12 h and passivation of surface by organic polymers such as PEG<sub>1500N</sub> or poly propionylethyleneimine-co-ethyleneimine (PPEI-EI). In another study, preparation of fluorescent CQDs *via* laser irradiation of a carbon suspension in organic solvent was reported by Hu et al. [46] (Figure 6(b)). To attain tunable light emission, the surface of CQDs could be altered by selecting proper organic solvents. Li et al. stated an easy laser ablation method to produce CQDs employing a common solvent as the liquid medium (such as acetone, ethanol or water) and nano-carbon materials (less than 50 nm) as the carbon precursor [5,45]. In this technique, first a suspension of 0.02 g of carbon nanomaterial in 50 ml ethanol was prepared which was afterwards sonicated for 10 min. Then 4 ml of the obtained mixture was poured into a glass cell for laser irradiation. A Nd:YAG pulsed laser (repetition rate 30 Hz, pulse width 8 ns, beam diameter 8 mm with  $\lambda_{\text{max}}=532$  nm) was applied to irradiate the suspension and the solution was then centrifuged (Figure 6(c)). As reported, the obtained CQDs exhibited tunable, visible and stable PL.

### Size control

Controlling the size of CQDs is a critical step to reach stable properties for specific applications. Up to now, numerous investigations have been done to attain uniform and homogeneous CQDs through synthesis or post-treatment. As reported in most of researches, the prepared CQDs particles

were refined through dialysis, filtration, gel-electrophoresis, column chromatography and centrifugation [8,34]. Also, uniform and tunable-size CQDs can be obtained employing limited pyrolysis of organic materials as precursor in nanoreactors [37] (Figure 7). This method can be divided into three steps as follows (i) impregnating silica spheres as nanoreactors with carbon precursor through capillary force, (ii) pyrolysing the confined carbon precursor and (iii) eliminating nanoreactors to release the obtained CQDs. In this method, pore diameter of porous nanoreactors is the most important parameter that determines the size and size distribution of final CQDs [37]. Porous silicas are common nanoreactors due to their thermal stability, tunability, availability of textures and easy removal [36,37].

Polymeric core-shell nanoparticles with thermally cross-linkable core and thermally removable shell are ideal alternatives for nanoreactors [47–49]. Wang et al. reported synthesis of uniformly n-doped CQDs by pyrolysis of poly acrylonitrile@poly methyl methacrylate (PAN@PMMA)-core-shell-nanoparticles obtained employing micro-emulsion polymerization procedure (Figure 8) [49]. The CQDs preparation process was as follows: the previously synthesized PAN@PMMA core-shell nanoparticles (1 ml) were heated at 270 °C for 2 h under a continuous air flow to cross-link the core domains (PAN part). Then the temperature was increased to 450 °C and held for 1 h to decompose the shell domains (PMMA part) and subsequently the final CQDs were carbonized. The obtained CQDs with average diameter of 2–3 nm exhibited a band gap-like PL behaviour, with dual emission and a stable PL between pH 5 and 12 [37].

To avoid carbonaceous accumulation during thermal treatment, thermally unstable polymers also could be employed

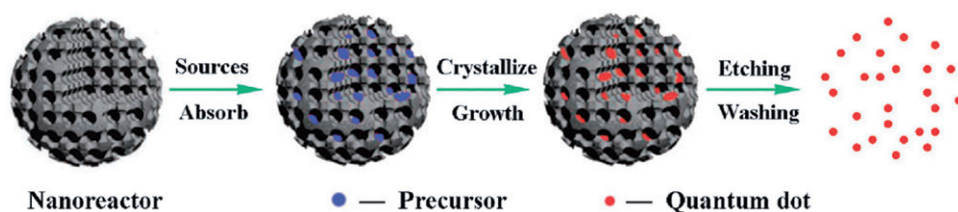


**Figure 7.** Schematic illustration of limited reaction in nanoreactors for synthesis of CQDs. (Reprinted from Ref. [37] with permission from The Royal Society of Chemistry).

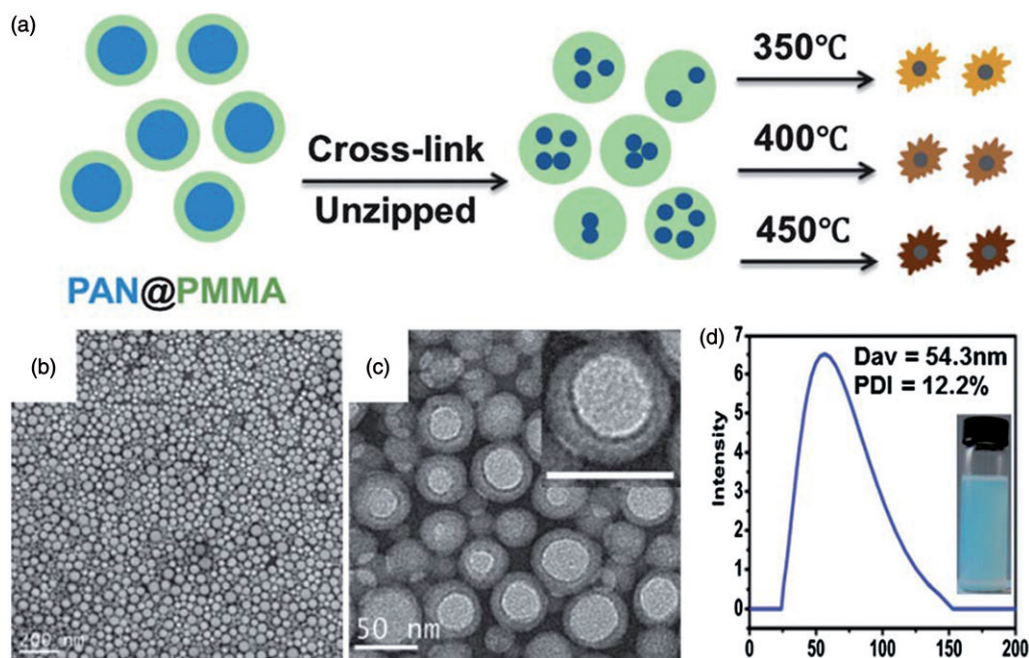


**Figure 8.** (a) Diagram of the synthesis of CQDs unzipped from PAN@PMMA core-shell nanoparticles. Numerous n-CQDs were unzipped from one polymeric nanoparticle and exhibited diverse PL behaviours at different pyrolysis temperatures. (b, c) TEM images of the PAN@PMMA core-shell nanoparticles. Scale bars are 200 nm (b) and 50 nm (c), respectively. (d) DLS curve of the PAN@PMMA core-shell nanoparticles; the inset exhibits a photograph of a PAN@PMMA microemulsion. (Reprinted from Ref. [49] with permission from The Royal Society of Chemistry).

as block material [50,51]. Recently, a new methodology to obtain narrowly-dispersed CQDs from size-tunable single chain polymeric nanoparticles, employing features of Bergman cyclization-intermediated chain collapse [52,53], was reported by Zhu et al. [51] (Figure 9). In this method, each CQD is produced from only one polymeric nanoparticle and each polymeric nanoparticle is responsible for producing its own CQD. This one-to-one correspondence is termed “bijective pairing”, in which size-tunable CQDs can be achieved by varying the carbon-rich components (enediyne-containing molecules) in polymeric nanoparticles. Interestingly, photoluminescent emission wavelength of CQDs showed red-shifts when the size of CQDs decreased, which an unusual behaviour compared to the other CQDs was prepared from the other sources.

Kang and coworkers developed a current-density controlled electrochemical technique, in which they obtained different sizes of CQDs by varying the applied current density from 10 to 200 mA cm<sup>-2</sup> in graphite rods (used as both cathode and anode) [30]. They showed low current density (20 mA cm<sup>-2</sup>) led to larger CQDs and increment in amount of CQDs emitting at longer wavelengths while high current density (180 mA cm<sup>-2</sup>) resulted in small CQDs and caused a blue shift in PL spectra. Figure 10(a) illustrates illumination of

four typical sizes of CQDs by white and UV light. The emitted colours of CQDs are strong and intense enough to be observed with the bare eyes. As we can see in Figure 10(c), the PL properties changed precisely with CQD size, where large CQDs (3.9 nm) gave N-IR emission, medium sized CQDs (1.6–3.2 nm) visible light emission (400–800 nm) and small CQDs (1.3 nm) UV light emission. They also carried out theoretical calculations to study the correlation between cluster size and luminescence clarifying why the obtained CQDs exhibited such intense emissions. They figured out that this phenomenon comes from the affiliation of HOMO–LUMO gap on the size of the CQDs. Increasing the size of CQDs causes decrement of HOMO–LUMO gap gradually and the gap energy shifts to visible-IR spectral range and vice versa.

### Surface modification

One of the most common techniques to change the surface properties of nanomaterials for particular applications is surface modification. In recent years, numerous investigations were performed for functionalizing and modifying the surface of CQDs including  $\pi$ - $\pi$  interactions [54], sol-gel [55,56], coordination [57] and covalent bonding [58,59]. CQDs have

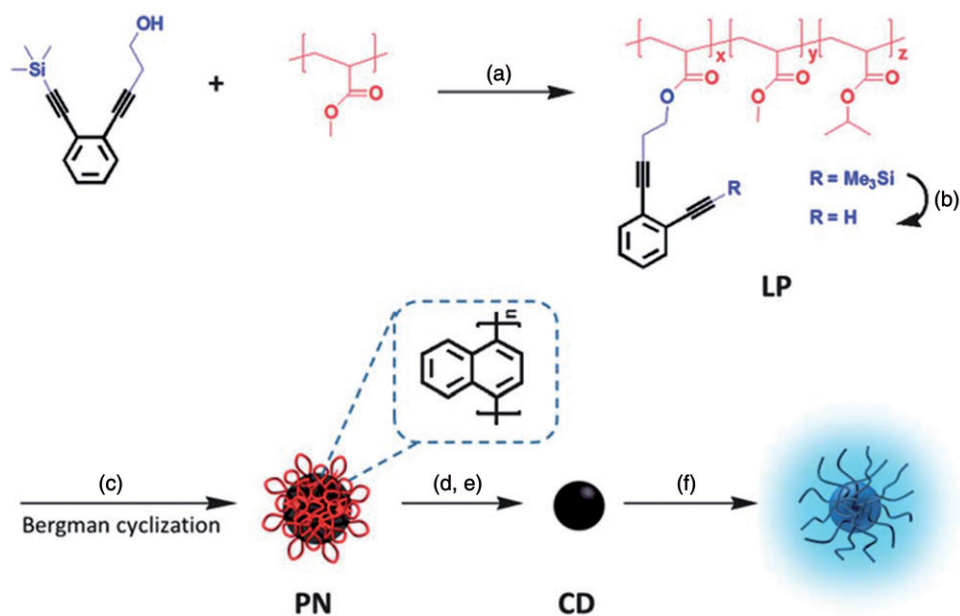


**Figure 9.** Schematic illustration of producing soluble CQDs with adjustable sizes from single-chain polymeric nanoparticles. (Reprinted from Ref. [51] with permission from The Royal Society of Chemistry).

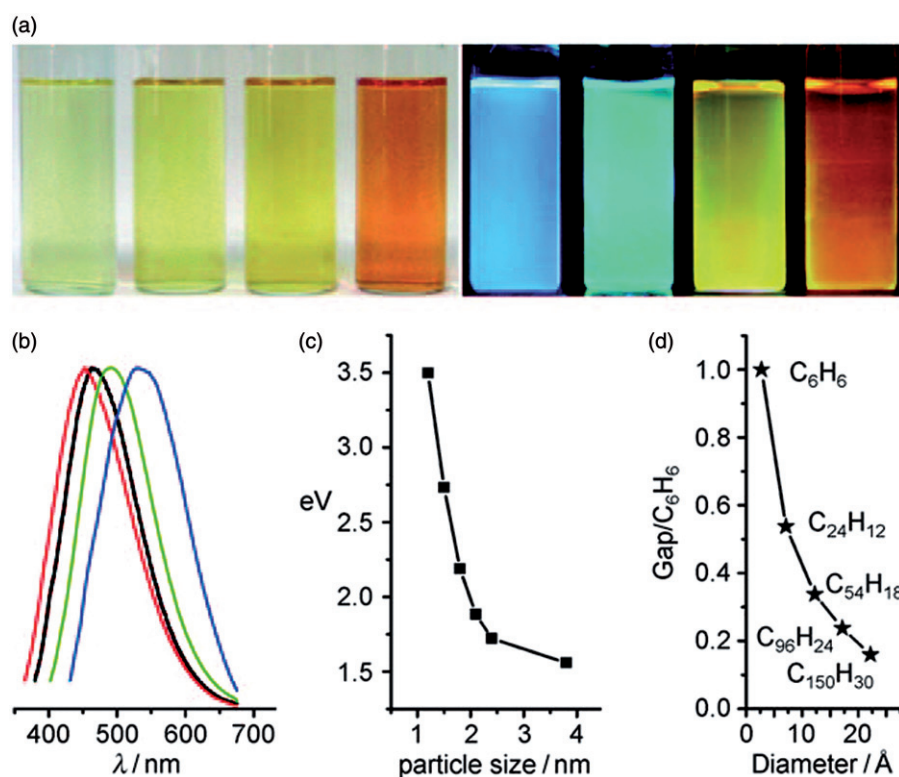


**Figure 10.** (a) Four typical sizes of CQDs illuminated by white (left; usual lamp; from left to right the colors are pale green, pale yellow, yellow and red, respectively) and UV light (right; 365 nm; from left to right the colors are blue, green, yellow and red, respectively); (b) four typical sizes of CQDs: from left to right the colors are red, black, green and blue lines are related to the PL spectra for blue-, green-, yellow- and red-emission CQDs, respectively; (c) correlation between PL properties and CQDs size; (d) the dependence of HOMO-LUMO gap on the size of the CQDs. (Reprinted from Ref. [30] with permission from Copyright 2010 John Wiley and Sons).

high amount of oxygen-containing groups that let them to covalently bind with other functional groups. Covalent bonding with chemical agents containing amine groups is a current approach for surface modification to reclaim the PL of CQDs, that proved to be very effective on changing the properties of CQDs. Three nm-CQDs which emitted blue-green light were modified with spiropyrans to achieve surface-

functionalized CQDs. The emission of the functionalized CQDs could be quenched at 510 nm, while being illuminated at 650 nm after irradiation with UV light and energy transferring between the CQDs and spiropyrans (Figure 11(a)) [60]. This process can be inverted by irradiation with visible light. High stability and excellent photo-reversibility are the main properties of these functionalized CQDs. The sol-gel method is

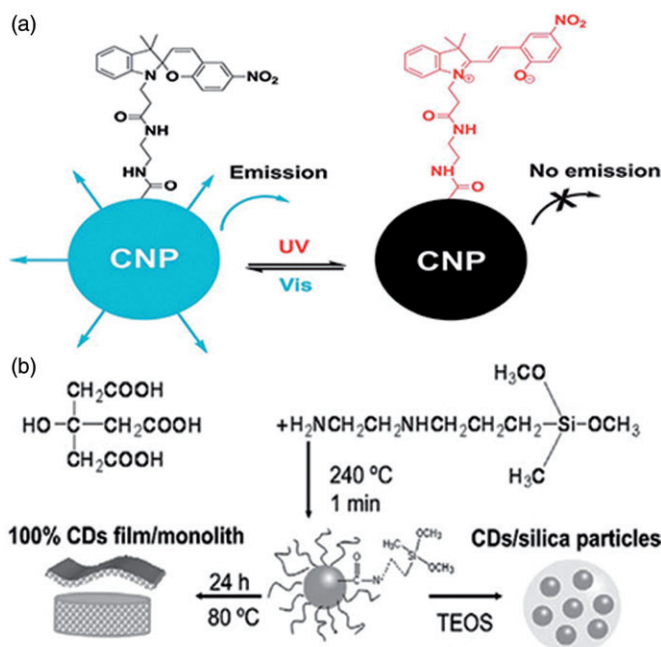


**Figure 11.** (a) Schematic representation of the light-excited fluorescence modulation of spiropyran-modified CQDs. (Reprinted from Ref. [60] with permission from The Royal Society of Chemistry.); (b) schematic diagram for the preparation of photoluminescent CQDs, flexible CD film and CQDs/silica particles. (Reprinted from Ref. [52] with permission from Copyright 2011 John Wiley and Sons).

another useful and promising strategy for modifying the surface of CQDs. Zhang and coworkers employed organosilane as a coordinating solvent to produce highly luminescent (QY = 47%) amorphous CQDs just in one minute [56]. As illustrated in Figure 11(b), the reaction proceeds through pyrolysis of anhydrous citric acid in *N*-( $\beta$ -aminoethyl)- $\gamma$ -aminopropyl methyltrimethoxy silane (AEAPMS) at 240 °C for 1 min. The surface of obtained CQDs (with average diameter of 0.9 nm) was enriched with methoxysilyl groups. Furthermore, the CQDs can easily be transformed into pure carbon dot (CD) fluorescent films or monoliths simply by heating them at 80 °C for 24 h [56]. Besides, the hydrophobic CQDs can be fabricated into hydrophilic silica-encapsulated CQDs (CQDs/silica), which showed no toxic behaviour in selected cell lines and were completely biocompatible. In a similar study, a CQDs@MIP (molecularly imprinted polymer) composite was applied as a molecular recognition element to construct dopamine (DA) FL optosensor [55]. Initially, AEAPMS was used as organosilane precursor to fabricate highly luminescent CQDs *via* a one-step hydrothermal reaction, and then their surfaces were anchored with MIP matrix to obtain CQDs@MIP composite. The obtained composite of a synergetic combination of CQDs with MIP exhibited high photo-stability and template selectivity. Furthermore, the composite showed a high sensitivity in detection of DA *via* FL intensity which decreases as original templates are removed [55].

## Properties

### Absorbance

CQDs usually have apparent optical absorption in the UV–visible region [7]. Most of the CQDs, no matter how they are synthesized, possess an absorption band around

260–323 nm. In some cases, the  $n\text{-}\pi^*$  transition of C=O bonds or the  $\pi\text{-}\pi^*$  transition of the C=C bonds may cause absorption shoulders in absorption spectra. It is found that surface passivation of CQDs with various molecules results in a shift of absorbance to longer wavelength.

### Photoluminescence

The size-dependent optical absorption or PL is the classic sign of quantum confinement, which is one of the most exciting features of CQDs. Since the results of studies on optical properties of CQDs are diverse and controversial, further clarification is required about exact mechanisms of PL. The clear reliance of the emission wavelength and intensity on  $\lambda_{\text{ex}}$  is one of the fascinating features of the PL of CQDs, whether it is because of various sizes of nanoparticles or diverse emissive traps that exist at the surface of CQDs. Zhao et al. asserted that the impact of size on excitation wavelength of CQDs PL was more than altering emissive trap sites on similar particles with the same size [61]. Furthermore, dispersal of diverse emissive sites on each particle may determine the optical behaviour of CQDs [7]. Sun et al. claimed that the presence of surface energy traps, which turn into emission upon surface passivation, attributes to the PL of CQDs. As they said, probably a quantum confinement impact of emissive energy traps on the surface is responsible for exhibiting strong PL upon surface passivation [62]. The CQDs produced by the supported technique required surface passivation to achieve strong PL emission (Figure 12) [22]. In this report, the presence of surface energy traps that turned into emission upon stabilization due to surface passivation causes bright and colourful PL from the CQDs. Therefore, in addition to different sizes of CQDs, dispersion of emissive trap sites at the surface

of CQDs leads to the colourful PL emission. Surface passivation is a critical step for the CQDs with size of 1.5–2 nm to attain PL property [22].

Li et al. reported that the source of the PL of prepared CQDs was due to carboxylate groups created at the surface of particle [45]. They claimed that some oxygen-containing radicals at the surface of the preliminary carbon precursors, produced by laser irradiation, would be the source of the PL. As they suggested, two factors were leading to tunable performance. The first factor was controlling the size of obtained particles similar to what was detected in semiconductor nanocrystals and the second was the diverse oxygen-containing groups. It turned out that, CQDs prepared by electrochemical oxidation technique employing MWCNTs exhibited blue PL and  $\lambda_{\text{ex}}$ -dependent emission whose PL does not need passivation step [26]. Li et al. produced CQDs from glucose as carbon precursor employing ultrasonic treatment technique [11]. Obtained CQDs showed N-IR emission after excitation by N-IR light which is very valuable for bioapplications due to the transparency of body tissues in this band known as

“water window” (Figure 13). The fabrication technique and the involved surface chemistry are the most significant factors that determine the QY of CQDs [7]. CQDs prepared by laser ablation with size of 5 nm had QY about 4–10% relying on the efficiency of the reaction on surface passivation and the excitation wavelength [63]. QY of 7 nm CQDs prepared by thermal decomposition methods was only 3% [12].

Interestingly, the CQDs which were linked with a metallic nanostructure or had a metal-containing shell, showed higher QY [64]. CQDs prepared by alkali-assisted electrochemical techniques exhibited good photostability which stayed still after one year of storage in air at room temperature [30]. It has been reported that pH value affects the CQDs PL intensity [65]. Zhao et al. reported that in very acidic or alkaline pH, the PL is nearly completely quenched. However, when the pH of the system was adjusted back to the range of 6.0–8.0, the FL intensity of the CQDs became high again [65].

### Electrochemical luminescence

ECL is a parameter which is widely applied to explore the fluorescent emission of semiconductor nanocrystals such as QDs [66] and nowadays have attracted researchers of CQDs [28]. Interestingly, ECL behaviour of QDs (such as CdSe) is similar to those of CQDs. We explain the ECL mechanism of CQDs as follows: first, with the potential cycle, the two states of oxidized ( $R^+$ ) and reduced ( $R^-$ ) of CQDs get formed. Then, the excited state ( $R^*$ ) is created after the electron-transfer eradication of the two oppositely charged carriers ( $R^+$  and  $R^-$ ). Lastly, by a radiative pathway through emitting a photon, the excited CQDs ( $R^*$  state) get returned to the ground state. It is good to know that the cathodic ECL strength was lower than the anodic one, implying that  $R^+$  was more unstable than  $R^-$ . Furthermore, due to stable ECL response over time, ECL sensing have recently found many applications and attracted researchers in the field. It is reported that when the cycled potential was between +1.8 and –1.5 V, strong ECL emission was detected from CQDs obtained from the electrochemical oxidation of graphite [28]. The surface states are the main origin for most ECL observed in semiconductor nanomaterials and is often meaningfully red shifted compared to PL peaks [67]. Since surface-state transitions in nanoparticles are mainly associated with ECL, to study the

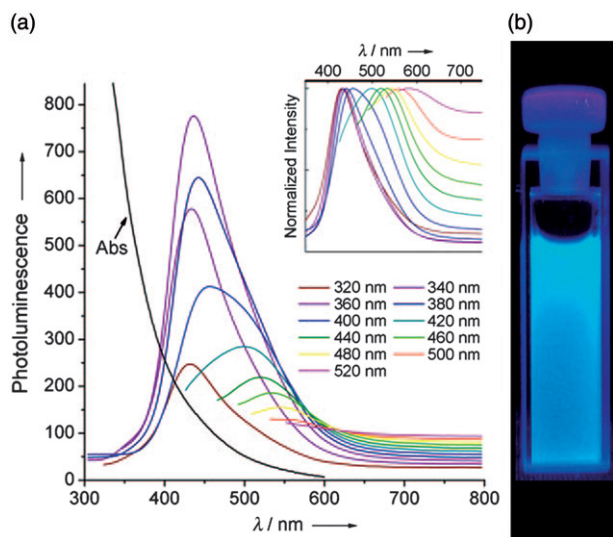


**Figure 12.** (a) Diagram illustration of UV/Vis absorption and PL emission spectra (recorded for increasingly longer excitation wavelengths from 320 to 520 nm in 20 nm increments) of CQDs surface-passivated with PEG<sub>1500N</sub> in water. In the inset, the emission spectral intensities are normalized. (b) Optical photograph attained under excitation at 365 nm. (Reprinted with permission from Ref. [22] Copyright 2009 John Wiley and Sons).

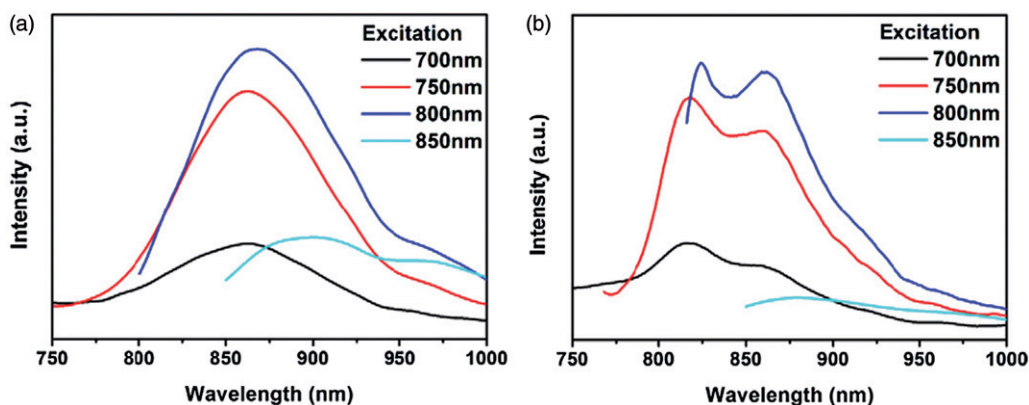


**Figure 13.** PL spectra of CQDs excited by N-IR (a) CQDs obtained from glucose/NaOH; (b) CQDs obtained from glucose/HCl. (Reprinted from Ref. [11] Copyright 2011, with permission from Elsevier).

presence of surface traps, it is very helpful to compare the ECL and PL of nanoparticles.

### Up-conversion photoluminescence (UCPL)

Due to the many promising applications of up-conversion FL materials, especially in biomedical imaging, they have attracted much recent attention. Until recent years, the UCPL of CQDs was mostly unclear. The multi-photon activation process is considered as the main reason of CQDs UCPL, in which absorption of multi photons (two or more photons) simultaneously, results in the emission of light with shorter wavelength than excitation light. The UCPL behaviour of CQDs provides new openings for cell imaging with two-photon luminescence microscopy. It is reported that when CQDs are excited by a femtosecond pulsed laser for two-photon excitation in the N-IR range (800–840 nm) or by an argon-ion laser (458 nm), they show strong emission in the visible region [14]. The one- and two-photon luminescence descriptions for the equal scanning region of CQDs are excellently matched (Figure 14). The UCPL properties of such CQDs have been proved by the representative two-photon luminescence spectrum. Kang et al. noticed that CQDs attained by an alkali-assisted electrochemical technique show excellent UCPL properties and size-dependent PL.

However, in a recent investigation, on five differently prepared CQDs with a FL spectrophotometer, it was confirmed that CQDs did not exhibit observable UCPL [68]. As they reported, normal FL excited by the leaking component from the second diffraction in the monochromator of the FL spectrophotometer was the actual derivation of the UCPL [68]. By inserting a proper long-pass filter in the excitation lane of a FL spectrophotometer, the leaking component and consequently UCPL can be eradicated. Most of experiments suggested that UCPL is actually the normal FL with linear response rather than a multiple phonon process and most of CQDs may not have observable UCPL. It is also critical to eliminate the normal FL when detecting upconversion FL [68].

### Cytotoxicity

Recently, wide range of investigations has been done in producing bio-probes based on bright CQDs with high stability.

Although, the serious issue for applications of functionalized CQDs in live tissues, cells, and animals is their biocompatibility. During the last few years, systematic cytotoxicity assessments were performed on both functionalized CQDs and pure CQDs. For cytotoxicity evaluations, Yung et al. produced CQDs, employing arc-discharge of graphite rods, which were afterwards refluxed in  $\text{HNO}_3$  for 12 h [42]. Apparently, unmodified CQDs were not toxic to cells up to  $0.4 \text{ mg ml}^{-1}$ . In another study on cytotoxicity, electrochemically prepared luminescent CQDs were evaluated by employing human kidney cell line, in which the CQDs showed no significant influence on cell viability [61]. Ray et al. introduced an improved soot-based method for preparation of CQDs in which the obtained CQDs, with diameters of 26 nm, had just insignificant cytotoxicity at required concentrations for FL bioimaging [10]. In terms of cytotoxicity assay, the CQDs modified with functional molecules, such as PAA (poly acrylic acid) [69], BPEI (branched poly ethylenimine) [70], PEI [71] and PEG [42] were evaluated. The CQDs which were coated with PEG in all available sizes were safe and biocompatible even in much higher concentrations than required for cell imaging and associated applications [72,73]. Furthermore, PEG<sub>1500N</sub>-modified CQDs were injected into mice and the results exhibited no substantial toxic effects *in vivo* up to 28 days [72]. In addition, CQDs functionalized with PPEI-EI, were significantly nonhazardous to the cells under a comparatively high CQD concentrations [14]. Based on MTT evaluation of pure PEI, it showed no toxic effect to HT-29 cells even at high concentrations. Yet CQDs modified with PEI were more toxic than PPEI-EI- modified CQDs apparently because of higher ethylenimine (EI) units in the PEI. Moreover, experimental results revealed that both free PAA and PAA-functionalized CQDs were damaging to cells even at low concentrations ( $50 \text{ mg ml}^{-1}$ ) and with low exposure time of 24 h. High-cytotoxic functional groups like BPEI under special circumstances such as low concentrations and short incubation time, still can be applied to functionalize CQDs [71]. All the results suggest that CQDs have much potential for *in vitro* and *in vivo* imaging studies and it is predicted that in near future CQDs will be replaced with common QDs and FDA-approved dyes applied as optical imaging agents.

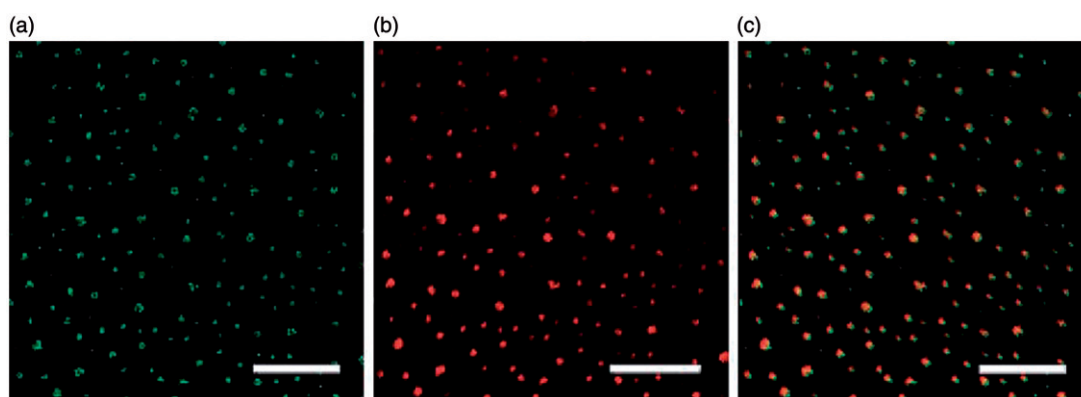


**Figure 14.** Luminescence images (all scale bars 20 nm) of the CQDs with (a) argon ion laser excitation at 458 nm and (b) femtosecond pulsed laser excitation at 800 nm; (c) is an overlap of (a) and (b). (Reprinted with permission from Ref. [14] Copyright (2007) American Chemical Society).

## Applications

### Bioimaging

CQDs possess great potential for fluorescent bioimaging due to their superior fluorescent properties, possibility of multi-modal bioimaging of cells and tissues, biocompatibility and low toxicity [74,75]. For the first time, the practicability of CQDs as a FL contrast agent was explored by Yang et al. [72]. Likewise, Sun et al. used PEGylated CQDs for *in vivo* optical imaging of different organs including bladder, kidney and liver (Figure 15) [42]. The images taken from the mice that were subcutaneously injected with PEGylated CQDs (440  $\mu\text{g}$  in 200  $\mu\text{L}$ ) had sufficient contrast. The injected CQDs, showed strong fluorescent *in vivo*, which combined with their biocompatibility, might offer great potential for optical imaging and related biomedical applications [42]. The same protocol was applied by Tao et al. in which FL images were collected at different wavelengths from 455 nm to 704 nm after subcutaneous injection of an aqueous solution of CQDs [76]. Multi-imaging is one of the most attractive technologies in which imaging probes are a combination of optical imaging and magnetic resonance imaging (MRI). Optical imaging permits for rapid screening whereas MRI has potential to concurrently attain physiological and anatomical information and provides high spatial resolution [77]. Recently, the preparation of ultrafine water-dispersible Gd(III)-doped CQDs with a dual MRI/FL character *via* the thermal decomposition has been reported [75]. The obtained particles showed bright FL in the visible area and displayed strong  $T_1$ -weighted MRI contrast with low cytotoxicity compared to commercial

Gadovist<sup>®</sup>. Therefore, the Gd-doped CQDs could be employed in biomedical research for multimodal imaging, where the MRI and FL modalities can be exploited simultaneously to improve image analysis. In another study, 6 nm iron oxide-doped CQDs (IO-CQDs) were produced *via* the pyrolysis of organic molecules as precursor in the presence of small  $\text{Fe}_3\text{O}_4$  nanoparticles for purpose of MR/FL multi-imaging [78]. IO-CQDs were injected intravenously into mice and results suggested observable FL signals in the spleen slide samples and contrast-enhanced MRI images under both  $T_1$  and  $T_2$  models. Besides, no significant cytotoxicity was observed and the nano-composite exhibited a biocompatible nature. The synthesized CQDs *via* hydrothermal carbonization of chitosan functionalized with amino groups were used for cyto-compatibility evaluation on A549 human lung adenocarcinoma cells [79]. Based on MTT assays, CQDs caused no significant toxicity and showed no influence on cell viability. So, relying on these results, CQDs are definitely applicable in high concentration for bioimaging applications [79].

### Photocatalysis

One of the important and also exiting fields in nano-chemistry is nano-photocatalysis, in which designing a strong nanocatalyst with tunable chemical activity is considered as the main object [80]. Photo-stability against photo-corrosion and being able to apply near UV and/or visible light are the major factors of a good photocatalyst. Specifically, CQDs with controlled sizes are capable of showing tunable emissions from blue wavelength to N-IR range which makes them

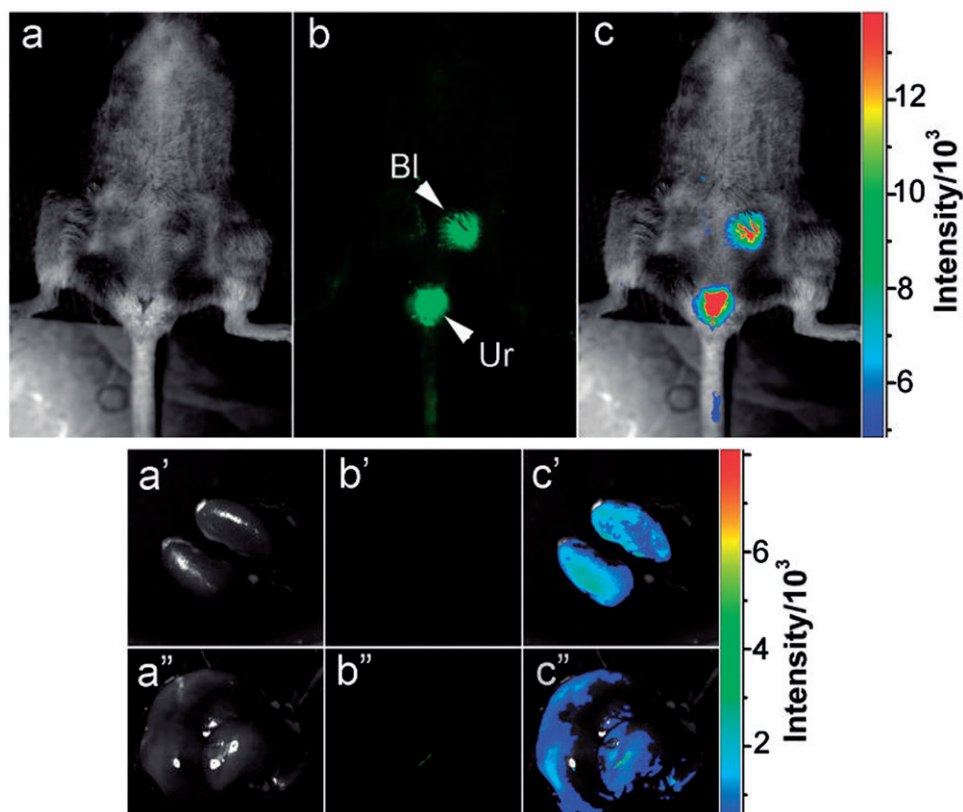


**Figure 15.** Intravenous injection of C-Dots: (a) bright field, (b) as-detected fluorescence (Bl, bladder; Ur, urine) and (c) colour-coded images. The same order is used for the images of the dissected kidneys (a'–c') and liver (a''–c''). (Reprinted with permission from Ref. [42] Copyright (2009) American Chemical Society).

promising candidates for photocatalysis. Lately, by one-step alkali-assisted electrochemical method, Kang and coworkers obtained 1.2–3.8 nm CQDs and designed a photocatalysis system based on  $\text{SiO}_2/\text{CQDs}$  and  $\text{TiO}_2/\text{CQDs}$  systems to make use of the full spectrum of sunlight (Figure 16) [30]. Due to up-conversion properties of this complex system, once CQDs absorb sun light (visible light), they emit the light in shorter wavelength (325–425 nm), which excites  $\text{SiO}_2$  or  $\text{TiO}_2$  to create electron/hole ( $e^-/h^+$ ) pairs (Figure 17). The reaction between the oxidants/reducers (such as  $\text{O}_2/\text{OH}^-$ ) and electron/hole pairs produces active oxygen radicals ( $\text{O}_2^-$ ,  $\text{OH}^-$ ) which results in degradation of the dyes (methyl blue, MB) [81]. Similarly, Zhang et al. reported designing of photocatalysts based on CQDs ( $\text{CQDs}/\text{Fe}_2\text{O}_3$ ) with excellent catalytic activity [82]. They claimed that the  $\text{CQDs}/\text{Fe}_2\text{O}_3$  nanocomposites have an incessant absorption band in the wavelengths around 550–800 nm and possess superior photocatalytic activity for the target reactions compared to  $\text{Fe}_2\text{O}_3$  alone.

Degradation analysis of methanol and gas-phase benzene suggests higher catalytic activity of  $\text{Fe}_2\text{O}_3/\text{CQDs}$  nanocomposites (80%) than  $\text{Fe}_2\text{O}_3$  nanoparticles (37%) alone in air atmosphere. Kang et al. believed that CQDs, by trapping electrons that emitted from  $\text{Fe}_2\text{O}_3$  nanoparticles and thereby lowering electron–hole recombination in the  $\text{Fe}_2\text{O}_3/\text{CQD}$  nanocomposites, play a crucial role in the high photocatalytic activity of the  $\text{Fe}_2\text{O}_3/\text{CQDs}$  nanocomposites.

In another study, preparation and catalytic activity of  $\text{CQDs}/\text{Ag}_3\text{PO}_4$  and  $\text{CQDs}/\text{Ag}/\text{Ag}_3\text{PO}_4$  complex as photocatalysis agents have been investigated [9]. Interestingly, both  $\text{CQDs}/\text{Ag}/\text{Ag}_3\text{PO}_4$  and  $\text{CQDs}/\text{Ag}_3\text{PO}_4$  nanocomposites, showed higher structural stability for methyl orange (MO) photo-degradation and greater photocatalytic activity than  $\text{Ag}_3\text{PO}_4$  alone. Protection of  $\text{Ag}_3\text{PO}_4$  from photo-corrosion is attributed to the CQDs which possess unique photoinduced electron transfer properties. Due to UCPL properties of the CQDs,  $\text{CQDs}/\text{Ag}_3\text{PO}_4$  and  $\text{CQDs}/\text{Ag}/\text{Ag}_3\text{PO}_4$ , they have great potential in using of full spectrum of sunlight which improves and enhances the photocatalytic activity. Furthermore, the creation rate of electron/hole pairs at the adjacent surface of

$\text{Ag}_3\text{PO}_4$  particles can further be enhanced due to surface plasmon resonance properties of Ag nanoparticles in the  $\text{CQDs}/\text{Ag}/\text{Ag}_3\text{PO}_4$  complex. In another recent investigation, Zhang et al. prepared water-soluble fluorescent n-doped CQDs (n-CQDs) by one-pot ultrasonic reaction amid ammonium hydroxide and glucose [9]. In addition to intense luminescence of the obtained n-CQDs in the visible to N-IR range and clear UCPL properties, they displayed good photocatalytic activity in the photodegradation of MO. CQDs have great potential in energy saving and green environment applications and may also be a promising choice for new generation of high-efficiency catalysts in energy technology and bioscience.

### Biosensor

Due to good biocompatibility, excitation-dependent multicolour emission, high photostability, superior cell permeability, good water solubility and surface modification capability of CQDs, they are promising candidate as biosensor agents. The biosensors based on CQDs could be applied for monitoring of various materials and parameters including cellular iron, copper, nucleic acid and pH [13]. As nucleic acid biosensing, CQDs can play an important role in biosensing science.

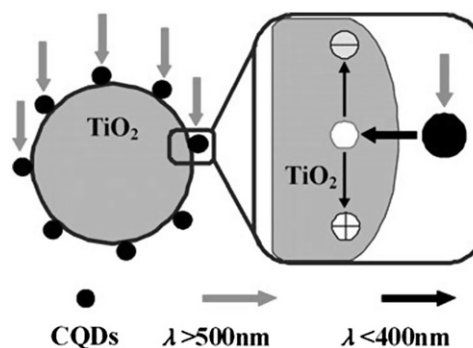


**Figure 17.** Illustration of catalytic mechanism for  $\text{TiO}_2/\text{CQDs}$  under visible daylight lamp. (Reprinted with permission from Ref. [30] Copyright 2010 John Wiley and Sons).

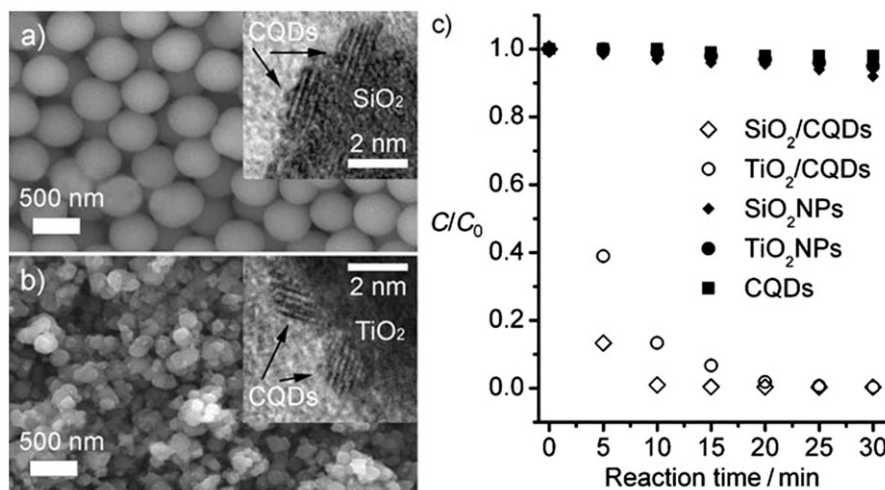


**Figure 16.** (a, b) SEM image of photocatalysts for  $\text{SiO}_2/\text{CQDs}$  and  $\text{TiO}_2/\text{CQDs}$ ; insets exhibit the corresponding HRTEM images; (c) correlation between MB concentration and reaction time for diverse catalysts:  $\text{SiO}_2/\text{CQDs}$ ,  $\text{TiO}_2/\text{CQDs}$ ,  $\text{SiO}_2$  NPs,  $\text{TiO}_2$  NPs and CQDs. (Reprinted with permission from Ref. [30] Copyright 2010 John Wiley and Sons).

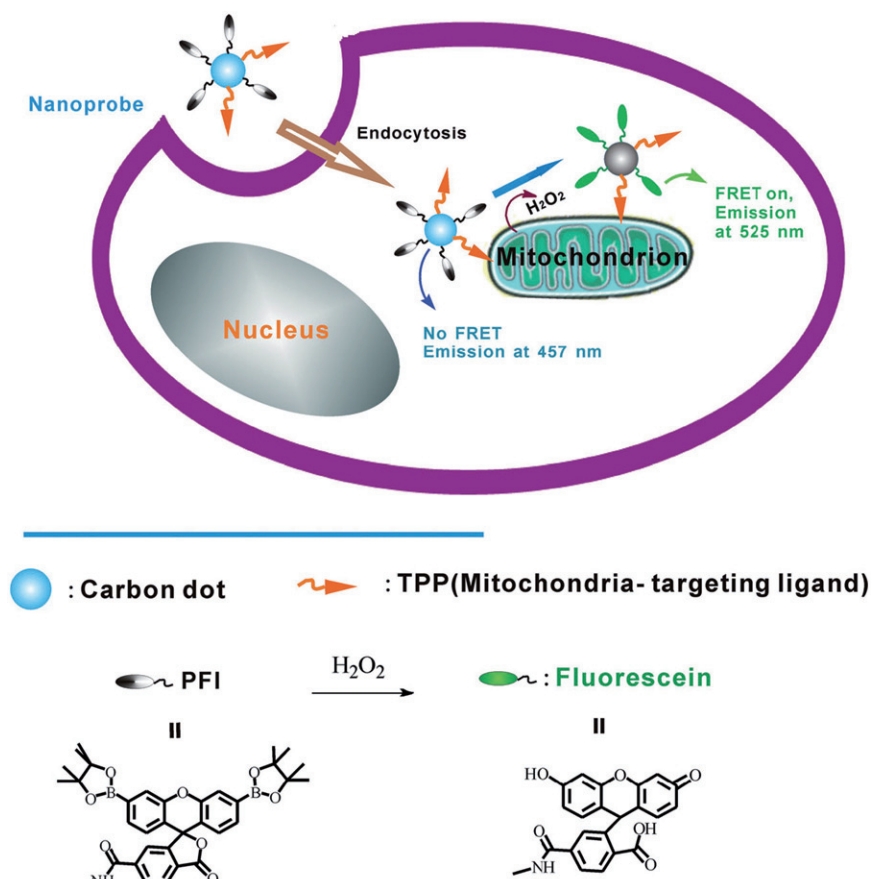


**Figure 18.** Graphical depiction of FRET-based ratiometric sensing of mitochondrial  $\text{H}_2\text{O}_2$  in living cell by the nano-probe. (Reprinted with permission from Ref. [83] Copyright 2013 John Wiley and Sons).

This system is based on adsorption of the fluorescent single-stranded DNA (ssDNA) probe by CQDs (as fluorescent quencher) *via*  $\pi$ - $\pi$  interactions. Once ssDNA is hybridized with its target and formed double-stranded DNA (dsDNA), desorption of the hybridized dsDNA from the CQDs surface and recovery of its FL, result in detecting the target DNA [54]. In another investigation, for sensing and imaging of mitochondrial  $\text{H}_2\text{O}_2$ , a strong and multifunctional FL resonance energy transfer (FRET) probe based on CQDs was exploited in which CQD acts as a carrier and giver of energy for detecting system [83]. In this study, the nano-probe was fabricated by covalently linking a mitochondria-targeting ligand, triphenylphosphonium (TPP), and an  $\text{H}_2\text{O}_2$  recognition element (PFI) onto CQDs (Figure 18). In the presence of  $\text{H}_2\text{O}_2$ , the PFI moieties on a CQD experiencing structural and spectral conversion, which represented the nanoplatform, a FRET-based ratiometric probe for  $\text{H}_2\text{O}_2$  [83]. Based on experimental results with a designed prob, fast and accurate detecting and measuring of exogenous  $\text{H}_2\text{O}_2$  levels in L929 cells have been possible. In another study, unfunctionalized CQDs with high sensitivity and selectivity were applied for detecting  $\text{Hg}^{2+}$  and biothiols [34]. This technique was based on FL quenching properties of  $\text{Hg}^{2+}$ , in which CQDs alone exhibited strong FL in aqueous environment while in the presence of  $\text{Hg}^{2+}$  the FL of CQDs was quenched. On the other hand,  $\text{Hg}^{2+}$ -S bonding formed due to presence of biothiols, which resulted in removal of  $\text{Hg}^{2+}$  from surface of CQDs and subsequently resulted in recovering of FL of CQDs. Thus, by monitoring of

FL intensity changes, a cheap, sensitive and selective FL sensor can be designed to detect presence of  $\text{Hg}^{2+}$  and biothiols. Based on same attitude, Qu et al. reported a similar route for CQD-based detection of  $\text{Fe}^{3+}$  and DA, in which  $\text{Fe}^{3+}$  can quench the CQDs by oxidizing the hydroquinone groups at the particles' surfaces and DA competes with CQDs to react with  $\text{Fe}^{3+}$  and protects CQDs from the FL quenching [5]. This operation just takes 10 min for detection of  $\text{Fe}^{3+}$  and DA which offers a rapid, selective and sensitive detection system. Dong et al. also designed a novel  $\text{Cu}^{2+}$  ion detection system based on poly(ethylenimine) (BPEI)-modified CQDs (BPEI-CQDs) [70]. In the obtained complex,  $\text{Cu}^{2+}$  ions could be caught by the amino groups at the surface of BPEI-CQDs, resulting in quenching the FL of CQDs through an inner filter effect. The designed complex was reported as a rapid, reliable and selective detection system for  $\text{Cu}^{2+}$  ions with detection limit as low as 6 nM and a dynamic range from 10 to 1100 nM. These CQD-based new strategies make us independent of QDs and organic dyes and we are able to apply more rapid, accurate, cost-effective and environment friendly methods.

### Drug delivery

In recent years, nanotechnology-based drug delivery systems (DDSs) have been widely developed and various nanomaterials such as graphene oxides [84], polymeric nanoparticles [85–87], MS [88–91] and AuNPs [92] have been investigated

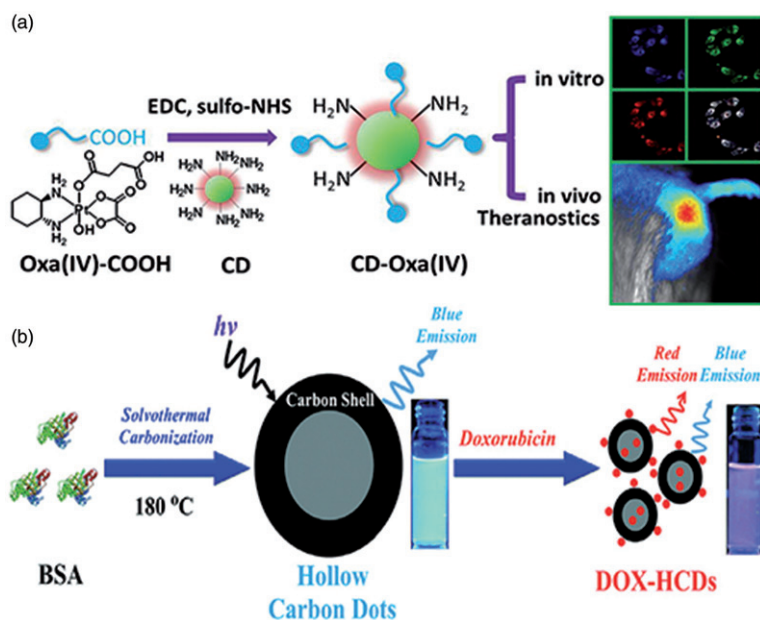


**Figure 19.** (a) Preparation procedure for CQDs-Oxa and its applications in bioimaging and theranostics. (Reprinted with permission from Ref. [92] Copyright 2014 John Wiley and Sons.); (b) graphical depiction of the preparation of luminescent HCQDs and the loading of DOX. (Reprinted from Ref. [16] Copyright 2013, with permission from Elsevier).

as drug delivery vehicles. AuNPs were the most investigated nanoparticles as DDSs, but due to their toxicity and biocompatibility issues they encountered various limits in clinical applications [93]. Due to fluorophore-quenching behaviour of AuNPs, they are difficult to track in *in vivo* systems [94] and also thiol groups are required on their surface for drug loading *via* Au–thiol interaction, which inflicts an additional limitation upon drug choice [95]. As mentioned before CQDs possess flexibility in surface modification with numerous chemicals molecules, high water solubility and excellent biocompatibility, therefore they could be excellent technological substitutes for AuNPs as a drug carriers [95]. Amongst platinum-based drugs, oxaliplatin is a comparatively novel platinum (II) complex that is currently being applied in a new, promising pharmacotherapy of metastatic colorectal cancer [96]. Due to side effects and drug resistance issues of Pt (II) complexes, it has been replaced with Pt (IV) complexes (Oxa (IV)-COOH) as a prodrug. Recently, Zheng et al. integrated oxidized oxaliplatin (Oxa (VI)-COOH) on the surface of CQDs by condensation reaction between the amino groups on the CQDs surface and the carboxyl group of Oxa (IV)-COOH *via* chemical coupling (CQDs-Oxa) (Figure 19(a)) [97]. CQDs-Oxa can be employed to diagnose, treat, and monitor response to therapy [97]. In cancer cells, drug was reduced upon the reduction of Oxa (IV)-COOH to oxaliplatin (II) after taking up CQDs-Oxa by cancer cells *via* endocytosis. It was revealed that, by monitoring the FL signal of the CQDs the distribution of the CQDs-Oxa can be tracked, which helps in estimating the proper dosage of the medicine and also injection time. In another study, Wang et al. synthesized doxorubicin (DOX)-loaded CQDs, which showed potential for application in both cell imaging and cancer therapy [16]. First, they prepared hollow CQDs (HCQDs) from bovine serum albumin (BSA) by solvothermal reaction (6.8 nm in diameter, pore size of 2 nm and QY = 7%) and then the produced particles were loaded with

DOX (Figure 19(b)). The sonicated solution of BSA (10 mg), ultrapure water (5 ml) and ethanol (10 ml) was heated at 180 °C for 12 h and then cooled to room temperature. HCQDs were centrifuged (12,000 rpm) and then added to DOX (0.1 mg ml<sup>-1</sup>) and stirred for a couple of hours for loading of DOX into HCQDs. Fluorescence images of A549 cells confirmed that HCQDs could be internalized by A549 cells and were mainly localized in the cytoplasm but could not enter the nucleus. Cell viability and cellular uptake results suggest that the HCQDs show low toxicity and act as a potential platform in drug delivery field. pH-triggered drug release, rapid cellular uptake, excitation-dependent PL and excellent biocompatibility were reported as the prominent advantages of designed HCQDs-based DDS [16]. Thakur et al. reported designing of antibiotic-conjugated CQDs *via* a microwave-assisted method using gum arabic (GA) as precursor, which used a theranostic agent for controlled drug release, bioimaging and enhanced antimicrobial activity [98]. In this work, CQDs served as a carrier for ciprofloxacin hydrochloride, a broad spectrum antibiotic, which was attached to the surface of synthesized CQDs (Cipro@CQDs). The Cipro@CQDs showed good biocompatibility on Vero cells as compared to free ciprofloxacin (1.2 mM) and ciprofloxacin release from CQDs depended extremely on physiological conditions [98]. Cipro@CQDs exhibited improved antimicrobial effect against both gram negative (*Escherichia coli*) and gram positive (*Staphylococcus aureus*) microorganisms and also showed bright green fluorescent when live imaging was applied to view yeast cells under fluorescent microscope.

## Outlook

In this article, recent developments in the field of CQDs, concentrating on their synthetic approaches, surface modification methods, various optical properties and their applications in

bioimaging, photocatalysis, biosensing and drug delivery have been discussed. The synthesis of CQDs is usually quite easy and only requires cheap and abundant materials. Furthermore, simple chemical experiments are needed for surface modification of CQDs that could be performed in a standard elementary level chemistry laboratory. Various size dependent optical properties of CQDs attracted scientists to examine and employ these particles in extensive applications which have been described. Compared to QDs, due to non-toxic behaviour of CQDs, they stand to have an enormous influence on environmental and biotechnological applications. Furthermore, because of excellent light absorbing ability of CQDs as well as their unique photo-induced electron transfer capability, they are considered as an excellent candidate for photocatalytic applications. High QY, high photo- and chemical-stability, beside non-blinking behaviour of CQDs encourage researchers to develop highly sensitive biosensors in different environments. CQDs have not been much investigated for their potential as a drug delivery vehicle, but because of all the above-mentioned properties, they are capable of being such efficient and promising vehicles. In the near future, we believe that CQDs will play a significant role in bioimaging, drug delivery and analytical science and the forthcoming studies must focus on CQDs as multifunctional agents, for instance acting as both bioimaging probe and catalyst at the same time. Moreover, in order to prevent public distrust and to address the risks and potential perils of emerging CQDs, novel techniques and tools should be established in order to identify and characterize their behaviours in biological matrices.

### Disclosure statement

No potential conflict of interest was reported by the authors.

### Funding

This work was funded by 2016 Drug Applied Research Center, Tabriz University of Medical Sciences Grant.

### References

- [1] Greiner NR, Phillips D, Johnson J, et al. Diamonds in detonation soot. *Nature*. 1988;333:440–442.
- [2] Liu Z, Zhou X, Qian Y. Synthetic methodologies for carbon nanomaterials. *Adv Mater Weinheim*. 2010;22:1963–1966.
- [3] Rao CN, Sood AK, Subrahmanyam KS, et al. Graphene: the new two-dimensional nanomaterial. *Angew Chem Int Ed*. 2009;48:7752–7777.
- [4] Yang W, Ratinac KR, Ringer SP, et al. Carbon nanomaterials in biosensors: should you use nanotubes or graphene? *Angew Chem Int Ed*. 2010;49:2114–2138.
- [5] Qu K, Wang J, Ren J, Qu X. Carbon dots prepared by hydrothermal treatment of dopamine as an effective fluorescent sensing platform for the label-free detection of iron(III) ions and dopamine. *Chemistry*. 2013;19:7243–7249.
- [6] Xu X, Ray R, Gu Y, et al. Electrophoretic analysis and purification of fluorescent single-walled carbon nanotube fragments. *J Am Chem Soc*. 2004;126:12736–12737.
- [7] Baker SN, Baker GA. Luminescent carbon nanodots: emergent nanolights. *Angew Chem Int Ed*. 2010;49:6726–6744.
- [8] Li H, Kang Z, Liu Y, et al. Carbon nanodots: synthesis, properties and applications. *J Mater Chem*. 2012;22:24230–24253.
- [9] Zhang H, Huang H, Ming H, et al. Carbon quantum dots/Ag<sub>3</sub>PO<sub>4</sub> complex photocatalysts with enhanced photocatalytic activity and stability under visible light. *J Mater Chem*. 2012;22:10501–10506.
- [10] Ray S, Saha A, Jana NR, et al. Fluorescent carbon nanoparticles: synthesis, characterization, and bioimaging application. *J Phys Chem C*. 2009;113:18546–18551.
- [11] Li H, He X, Liu Y, et al. One-step ultrasonic synthesis of water-soluble carbon nanoparticles with excellent photoluminescent properties. *Carbon*. 2011;49:605–609.
- [12] Bourlinos AB, Stassinopoulos A, Anglos D, et al. Surface functionalized carbogenic quantum dots. *Small*. 2008;4:455–458.
- [13] da Silva JCE, Gonçalves HM. Analytical and bioanalytical applications of carbon dots. *TrAC Trends Anal Chem*. 2011;30:1327–1336.
- [14] Cao L, Wang X, Mezziani MJ, et al. Carbon dots for multiphoton bioimaging. *J Am Chem Soc*. 2007;129:11318–11319.
- [15] Yu H, Shi R, Zhao Y, et al. Smart utilization of carbon dots in semiconductor photocatalysis. *Adv Mater*. 2016;28:9454–9477.
- [16] Wang Q, Huang X, Long Y, et al. Hollow luminescent carbon dots for drug delivery. *Carbon*. 2013;59:192–199.
- [17] Lin X, Yang Y, Nian L, et al. Interfacial modification layers based on carbon dots for efficient inverted polymer solar cells exceeding 10% power conversion efficiency. *Nano Energy*. 2016;26:216–223.
- [18] Lu S, Cong R, Zhu S, et al. pH-dependent synthesis of novel structure-controllable polymer-carbon nanodots with high acidophilic luminescence and super carbon dots assembly for white light-emitting diodes. *ACS Appl Mater Interfaces*. 2016;8:4062–4068.
- [19] Wang D, Wang Z, Zhan Q, et al. Facile and scalable preparation of fluorescent carbon dots for multifunctional applications. *Engineering*. 2017;3:402–408.
- [20] Bao L, Liu C, Zhang ZL, et al. Photoluminescence-tunable carbon nanodots: surface-state energy-gap tuning. *Adv Mater*. 2015;27:1663–1667.
- [21] Shen L, Zhang L, Chen M, et al. The production of pH-sensitive photoluminescent carbon nanoparticles by the carbonization of polyethylenimine and their use for bioimaging. *Carbon*. 2013;55:343–349.
- [22] Liu R, Wu D, Liu S, et al. An aqueous route to multicolor photoluminescent carbon dots using silica spheres as carriers. *Angew Chem*. 2009;121:4668–4671.
- [23] Liu Y, Xiao N, Gong N, et al. One-step microwave-assisted polyol synthesis of green luminescent carbon dots as optical nanoprobes. *Carbon*. 2014;68:258–264.
- [24] Castro HP, Souza VS, Scholten JD, et al. Synthesis and characterisation of fluorescent carbon nanodots produced in ionic liquids by laser ablation. *Chem Eur J*. 2016;22:138–143.
- [25] Hu C, Yu C, Li M, et al. Chemically tailoring coal to fluorescent carbon dots with tuned size and their capacity for Cu(II) detection. *Small*. 2014;10:4926–4933.
- [26] Zhou J, Booker C, Li R, et al. An electrochemical avenue to blue luminescent nanocrystals from multiwalled carbon nanotubes (MWCNTs). *J Am Chem Soc*. 2007;129:744–745.
- [27] Zhao Z, Xie Y. Enhanced electrochemical performance of carbon quantum dots-polyaniline hybrid. *J Power Sources*. 2017;337:54–64.
- [28] Zheng L, Chi Y, Dong Y, et al. Electrochemiluminescence of water-soluble carbon nanocrystals released electrochemically from graphite. *J Am Chem Soc*. 2009;131:4564–4565.
- [29] Lu J, Yang J-x, Wang J, et al. One-pot synthesis of fluorescent carbon nanoribbons, nanoparticles, and graphene by the exfoliation of graphite in ionic liquids. *ACS Nano*. 2009;3:2367–2375.
- [30] Li H, He X, Kang Z, et al. Water-soluble fluorescent carbon quantum dots and photocatalyst design. *Angew Chem Int Ed*. 2010;49:4430–4434.
- [31] Canevari TC, Nakamura M, Cincotto FH, et al. High performance electrochemical sensors for dopamine and epinephrine using nanocrystalline carbon quantum dots obtained under controlled chronoamperometric conditions. *Electrochim Acta*. 2016;209:464–470.

- [32] Hou Y, Lu Q, Deng J, et al. One-pot electrochemical synthesis of functionalized fluorescent carbon dots and their selective sensing for mercury ion. *Anal Chim Acta*. 2015;866:69–74.
- [33] Dong Y, Zhou N, Lin X, et al. Extraction of electrochemiluminescent oxidized carbon quantum dots from activated carbon. *Chem Mater*. 2010;22:5895–5899.
- [34] Qiao Z-A, Wang Y, Gao Y, et al. Commercially activated carbon as the source for producing multicolor photoluminescent carbon dots by chemical oxidation. *Chem Commun*. 2010;46:8812–8814.
- [35] Peng H, Travas-Sejdic J. Simple aqueous solution route to luminescent carbogenic dots from carbohydrates. *Chem Mater*. 2009;21:5563–5565.
- [36] Bourlinos AB, Stassinopoulos A, Anglos D, et al. Photoluminescent carbogenic dots. *Chem Mater*. 2008;20:4539–4541.
- [37] Zong J, Zhu Y, Yang X, et al. Synthesis of photoluminescent carbogenic dots using mesoporous silica spheres as nanoreactors. *Chem Commun*. 2011;47:764–766.
- [38] Edison TNJI, Atchudan R, Sethuraman MG, et al. Microwave assisted green synthesis of fluorescent N-doped carbon dots: cytotoxicity and bio-imaging applications. *J Photochem Photobiol B: Biol*. 2016;161:154–161.
- [39] Wang L, Bi Y, Hou J, et al. Facile, green and clean one-step synthesis of carbon dots from wool: application as a sensor for glyphosate detection based on the inner filter effect. *Talanta*. 2016;160:268–275.
- [40] Yang X, Yang X, Li Z, et al. Photoluminescent carbon dots synthesized by microwave treatment for selective image of cancer cells. *J Colloid Interface Sci*. 2015;456:1–6.
- [41] Tang L, Ji R, Cao X, et al. Deep ultraviolet photoluminescence of water-soluble self-passivated graphene quantum dots. *ACS Nano*. 2012;6:5102–5110.
- [42] Yang S-T, Cao L, Luo PG, et al. Carbon dots for optical imaging in vivo. *J Am Chem Soc*. 2009;131:11308–11309.
- [43] Wang X, Cao L, Lu F, et al. Photoinduced electron transfers with carbon dots. *Chem Commun*. 2009;(25):3774–3776.
- [44] Gonçalves H, da Silva JCE. Fluorescent carbon dots capped with PEG200 and mercaptosuccinic acid. *J Fluoresc*. 2010;20:1023–1028.
- [45] Li X, Shimizu H, Pyatenko Y, et al. Preparation of carbon quantum dots with tunable photoluminescence by rapid laser passivation in ordinary organic solvents. *Chem Commun*. 2010;47:932–934.
- [46] Hu S-L, Niu K-Y, Sun J, et al. One-step synthesis of fluorescent carbon nanoparticles by laser irradiation. *J Mater Chem*. 2009;19:484–488.
- [47] Guo X, Wang C-F, Yu Z-Y, et al. Facile access to versatile fluorescent carbon dots toward light-emitting diodes. *Chem Commun*. 2012;48:2692–2694.
- [48] Tang Qi CK, Wooley K, Matyjaszewski LK, et al. Well-defined carbon nanoparticles prepared from water-soluble shell cross-linked micelles that contain polyacrylonitrile cores. *Angew Chem Int Ed*. 2004;43:2783–2787.
- [49] Wang Y, Dong L, Xiong R, et al. Practical access to bandgap-like N-doped carbon dots with dual emission unzipped from PAN@PMMA core-shell nanoparticles. *J Mater Chem C*. 2013;1:7731–7735.
- [50] Mackay ME, Tuteja A, Duxbury PM, et al. General strategies for nanoparticle dispersion. *Science*. 2006;311:1740–1743.
- [51] Zhu B, Sun S, Wang Y, et al. Preparation of carbon nanodots from single chain polymeric nanoparticles and theoretical investigation of the photoluminescence mechanism. *J Mater Chem C*. 2013;1:580–586.
- [52] Xiao Y, Hu A. Bergman cyclization in polymer chemistry and material science. *Macromol Rapid Commun*. 2011;32:1688–1698.
- [53] Zhu B, Ma J, Li Z, et al. Formation of polymeric nanoparticles via Bergman cyclization mediated intramolecular chain collapse. *J Mater Chem*. 2011;21:2679–2683.
- [54] Li H, Zhang Y, Wang L, et al. Nucleic acid detection using carbon nanoparticles as a fluorescent sensing platform. *Chem Commun*. 2011;47:961–963.
- [55] Mao Y, Bao Y, Han D, et al. Efficient one-pot synthesis of molecularly imprinted silica nanospheres embedded carbon dots for fluorescent dopamine optosensing. *Biosens Bioelectron*. 2012;38:55–60.
- [56] Wang F, Xie Z, Zhang H, et al. Highly luminescent organosilane-functionalized carbon dots. *Adv Funct Mater*. 2011;21:1027–1031.
- [57] Zhao HX, Liu LQ, De Liu Z, et al. Highly selective detection of phosphate in very complicated matrixes with an off-on fluorescent probe of europium-adjusted carbon dots. *Chem Commun*. 2011;47:2604–2606.
- [58] Dong Y, Wang R, Li H, et al. Polyamine-functionalized carbon quantum dots for chemical sensing. *Carbon*. 2012;50:2810–2815.
- [59] Yin J-Y, Liu H-J, Jiang S, et al. Hyperbranched polymer functionalized carbon dots with multistimuli-responsive property. *ACS Macro Lett*. 2013;2:1033–1037.
- [60] Liao B, Long P, He B, et al. Reversible fluorescence modulation of spiropyran-functionalized carbon nanoparticles. *J Mater Chem C*. 2013;1:3716–3721.
- [61] Zhao Q-L, Zhang Z-L, Huang B-H, et al. Facile preparation of low cytotoxicity fluorescent carbon nanocrystals by electrooxidation of graphite. *Chem Commun*. 2008;(41):5116–5118.
- [62] Wilson WL, Szajowski P, Brus L. Quantum confinement in size-selected, surface-oxidized silicon nanocrystals. *Science*. 1993;262:1242.
- [63] Sun Y-P, Zhou B, Lin Y, et al. Quantum-sized carbon dots for bright and colorful photoluminescence. *J Am Chem Soc*. 2006;128:7756–7757.
- [64] Tian L, Ghosh D, Chen W, et al. Nanosized carbon particles from natural gas soot. *Chem Mater*. 2009;21:2803–2809.
- [65] Li H, Ming H, Liu Y, et al. Fluorescent carbon nanoparticles: electrochemical synthesis and their pH sensitive photoluminescence properties. *New J Chem*. 2011;35:2666–2670.
- [66] Qi H, Peng Y, Gao Q, et al. Applications of nanomaterials in electrogenerated chemiluminescence biosensors. *Sensors*. 2009;9:674–695.
- [67] Ding Z, Quinn BM, Haram SK, et al. Electrochemistry and electro-generated chemiluminescence from silicon nanocrystal quantum dots. *Science*. 2002;296:1293–1297.
- [68] Wen X, Yu P, Toh Y-R, et al. On the upconversion fluorescence in carbon nanodots and graphene quantum dots. *Chem Commun (Camb)*. 2014;50:4703–4706.
- [69] Wang Y, Bao L, Liu Z, et al. Aptamer biosensor based on fluorescence resonance energy transfer from upconverting phosphors to carbon nanoparticles for thrombin detection in human plasma. *Anal Chem*. 2011;83:8130–8137.
- [70] Dong Y, Wang R, Li G, et al. Polyamine-functionalized carbon quantum dots as fluorescent probes for selective and sensitive detection of copper ions. *Anal Chem*. 2012;84:6220–6224.
- [71] WangAnilkumar Y, Cao PL, Liu J-H, et al. Carbon dots of different composition and surface functionalization: cytotoxicity issues relevant to fluorescence cell imaging. *Exp Biol Med*. 2011;236:1231–1238.
- [72] Yang S-T, Wang X, Wang H, et al. Carbon dots as nontoxic and high-performance fluorescence imaging agents. *J Phys Chem C Nanomater Interfaces*. 2009;113:18110–18114.
- [73] Wang X, Cao L, Yang ST, et al. Bandgap-like strong fluorescence in functionalized carbon nanoparticles. *Angew Chem*. 2010;122:5438–5442.
- [74] Bhunia SK, Saha A, Maity AR, et al. Carbon nanoparticle-based fluorescent bioimaging probes. *Sci Rep*. 2013;3:1473.
- [75] Bourlinos AB, Bakandritsos A, Kouloumpis A, et al. Gd (III)-doped carbon dots as a dual fluorescent-MRI probe. *J Mater Chem*. 2012;22:23327–23330.
- [76] Tao H, Yang K, Ma Z, et al. In vivo NIR fluorescence imaging, biodistribution, and toxicology of photoluminescent carbon dots produced from carbon nanotubes and graphite. *Small*. 2012;8:281–290.
- [77] Lee D-E, Koo H, Sun I-C, et al. Multifunctional nanoparticles for multimodal imaging and theragnosis. *Chem Soc Rev*. 2012;41:2656–2672.

- [78] Srivastava S, Awasthi R, Tripathi D, et al. Magnetic-nanoparticle-doped carbogenic nanocomposite: an effective magnetic resonance/fluorescence multimodal imaging probe. *Small*. 2012;8:1099–1109.
- [79] Yang Y, Cui J, Zheng M, et al. One-step synthesis of amino-functionalized fluorescent carbon nanoparticles by hydrothermal carbonization of chitosan. *Chem Commun*. 2012;48:380–382.
- [80] Turner M, Golovko VB, Vaughan OP, et al. Selective oxidation with dioxygen by gold nanoparticle catalysts derived from 55-atom clusters. *Nature*. 2008;454:981–983.
- [81] Li J, Ma W, Chen C, et al. Photodegradation of dye pollutants on one-dimensional TiO<sub>2</sub> nanoparticles under UV and visible irradiation. *J Mol Catal A: Chem*. 2007;261:131–138.
- [82] ZhangMing H, Lian H, Huang S, et al. Fe<sub>2</sub>O<sub>3</sub>/carbon quantum dots complex photocatalysts and their enhanced photocatalytic activity under visible light. *Dalton Trans*. 2011;40:10822–10825.
- [83] Du F, Min Y, Zeng F, et al. A targeted and FRET-based ratiometric fluorescent nanoprobe for imaging mitochondrial hydrogen peroxide in living cells. *Small*. 2014;10:964–972.
- [84] Sun X, Liu Z, Welsher K, et al. Nano-graphene oxide for cellular imaging and drug delivery. *Nano Res*. 2008;1:203–212.
- [85] Salehi R, Arsalani N, Davaran S, et al. Synthesis and characterization of thermosensitive and pH-sensitive poly (N-isopropylacrylamide-acrylamide-vinylpyrrolidone) for use in controlled release of naltrexone. *J Biomed Mater Res*. 2009;89:919–928.
- [86] Zeighamian V, Darabi M, Akbarzadeh A, et al. PNIPAAm-MAA nanoparticles as delivery vehicles for curcumin against MCF-7 breast cancer cells. *Artif Cells Nanomed Biotechnol*. 2016;44:735–742.
- [87] Rahmani Del Bakhshayesh A, Annabi N, Khalilov R, et al. Recent advances on biomedical applications of scaffolds in wound healing and dermal tissue engineering. *Artif Cells Nanomed Biotechnol*. Forthcoming. [cited 2017 Jul 12]. doi: 10.1080/21691401.2017.1349778
- [88] Rasouli S, Davaran S, Rasouli F, et al. Positively charged functionalized silica nanoparticles as nontoxic carriers for triggered anticancer drug release. *Design Monom Polym*. 2014;17:227–237.
- [89] Alidadiyani N, Salehi R, Ghaderi S, et al. Synergistic antiproliferative effects of methotrexate-loaded smart silica nanocomposites in MDA-MB-231 breast cancer cells. *Artif Cells Nanomed Biotechnol*. 2016;44:603–609.
- [90] Salehi R, Davaran S, Hamishekar H. Functionalized cationic silica nanoparticles as biocompatible carriers by stimuli-responsive nanovalves as double anticancer drug delivery systems. 1st Tabriz International Life Science Conference and 12th Iran Biophysical Chemistry Conference; 2013.
- [91] Shabestari Khiabani S, Farshbaf M, Akbarzadeh A, et al. Magnetic nanoparticles: preparation methods, applications in cancer diagnosis and cancer therapy. *Artif Cells Nanomed Biotechnol*. 2017;45:6–17.
- [92] Panahi Y, Mohammadhosseini M, Nejati-Koshki K, et al. Preparation, surface properties, and therapeutic applications of gold nanoparticles in biomedicine. *Drug Res*. 2017;67:77–87.
- [93] Alkilany AM, Murphy CJ. Toxicity and cellular uptake of gold nanoparticles: what we have learned so far? *J Nanopart Res*. 2010;12:2313–2333.
- [94] Dulkeith E, Morteaux A, Niedereichholz T, et al. Fluorescence quenching of dye molecules near gold nanoparticles: radiative and nonradiative effects. *Phys Rev Lett*. 2002; 89:203002.
- [95] Kumar V, Toffoli G, Rizzolio F. Fluorescent carbon nanoparticles in medicine for cancer therapy. *ACS Med Chem Lett*. 2013; 4:1012–1013.
- [96] Alcindor T, Beauger N. Oxaliplatin: a review in the era of molecularly targeted therapy. *Curr Oncol*. 2011;18:18–25.
- [97] Zheng M, Liu S, Li J, et al. Integrating oxaliplatin with highly luminescent carbon dots: an unprecedented theranostic agent for personalized medicine. *Adv Mater*. 2014;26:3554–3560.
- [98] Thakur M, Pandey S, Mewada A, et al. Antibiotic conjugated fluorescent carbon dots as a theranostic agent for controlled drug release, bioimaging, and enhanced antimicrobial activity. *J Drug Deliv*. 2014;2014:282193.